# NATIONAL ADVISORY COMMITTEE FOR AERONAUTICS

**TECHNICAL NOTE 2053**

# EFFECT OF HEAT AND POWER EXTRACTION ON TURBOJET-ENGINE PERFORMANCE. I - ANALYTICAL METHOD OF PERFORMANCE EVALUATION WITH COMPRESSOR-OUTLET AIR BLEED

By Reece V. Hensley, Frank E. Rom
and Stanley L. Koutz

Lewis Flight Propulsion Laboratory
Cleveland, Ohio


Washington
March 1950

NATIONAL ADVISORY COMMITTEE FOR AERONAUTICS

TECHNICAL NOTE 2053

# EFFECT OF HEAT AND POWER EXTRACTION ON TURBOJET-ENGINE PERFORMANCE. I - ANALYTICAL METHOD OF PERFORMANCE EVALUATION WITH COMPRESSOR-OUTLET AIR BLEED

By Reece V. Hensley, Frank E. Rom
and Stanley L. Koutz

## SUMMARY

The performance of a turbojet engine with air bled off at the compressor outlet is analytically investigated. The analysis is based on the experimentally determined characteristics of the components of a typical axial-flow-type turbojet engine. Changes in the matching characteristics of the engine components and the change of the mass of working fluid within the cycle are accounted for in the analysis. A wide range of engine and flight conditions is covered and air bleeds from 0 to 15 percent of the air mass flow through the compressor are considered.

The results are presented in nondimensional form to facilitate their application to different engines and are applicable for turbojet engines with pressure ratios of 4 to 5 and turbine-inlet temperatures of approximately 2000° R. For engines outside this range as well as for centrifugal-flow-type engines, the method for calculating the effect of air bleed as set forth in this analysis is still applicable. Results of the analysis are presented both as functions of the pressure and temperature ratios across the engine and in terms of the conventional propulsion-system characteristics in corrected form: engine speed, turbine-inlet temperature, tail-pipe-nozzle area, thrust, and specific fuel consumption.

In the course of the analysis, it was found that the over-all engine temperature and pressure ratios were extremely sensitive to the tail-pipe-nozzle area and the prediction of constant-area performance was consequently difficult. If any given variation of tail-pipe temperature with air bleed is used, however, such as holding tail-pipe temperature constant, excellent checks are obtained between the experimental and analytical performance of axial-flow-type turbojet engines with air bleed.

## INTRODUCTION

In the operation of current and future aircraft, considerable quantities of compressed air may be required for such uses as cabin pressurization and conditioning, protection against ice formation, and boundary-layer control. The compressed air can be obtained from auxiliary equipment; such equipment, however, requires space and reduces the pay-load capacity of the airplane. In addition to these disadvantages, the auxiliary equipment must be designed for peak loads that occur only for small fractions of the total flight time.

If the airplane is powered by a gas-turbine engine, the amount of auxiliary equipment needed can be reduced by bleeding air from the compressor outlet. Although this system has the advantage of requiring a minimum of additional weight and space, bleeding air from the engine will adversely affect the engine performance.

As part of a program being conducted at the NACA Lewis laboratory to evaluate the various means for obtaining auxiliary power in aircraft, the effect of bleeding air from the compressor outlet of an axial-flow turbojet engine has been investigated. Two main phases are considered: (1) the method of analysis and the development of generalized performance charts for a turbojet engine with air bleed; and (2) the effect of air bleed on specific modes of engine operation.

The analysis, which is based on experimentally determined component characteristics derived from an analysis of unavailable data obtained during altitude-wind-tunnel investigations of a complete turbojet engine with several tail-pipe nozzles, is presented herein. The characteristics were idealized by fairing a single curve through the data for several ram pressure ratios and altitudes.

The performance of the basic turbojet engine (combination of compressor, combustion chamber, and turbine) is determined from the individual component characteristics by the matching procedure of reference 1. The matching procedure involves the simultaneous evaluation of compressor and turbine variables such as speed, mass flow, pressure ratio, and temperature ratio and the combustion-chamber temperature and pressure ratios. Bleeding air from the compressor outlet changes these variables and consequently changes the basic engine performance. Changes in the matching of the components as well as changes in the mass flow are taken into account in the analysis. The performance of the basic engine, as determined from the matching procedure, is presented in the form of pumping

characteristics (reference 2). The mass flow through the engine is given herein as a function of engine speed; the over-all engine pressure ratio is given as a function of over-all engine temperature ratio, engine speed, and air-bleed ratio.

The performance characteristics of the complete propulsion system are obtained by matching the characteristics of the engine-inlet system, the basic engine, and the tail-pipe nozzle. The effect of air bleed on propulsion-system performance is presented in the form of generalized propulsion-system performance parameters from which various problems involving air bleed can be solved.

## SYMBOLS

The following symbols are used in this analysis:

| | |
|---|---|
| $A$ | area, square feet |
| $C_d$ | discharge coefficient |
| $c_p$ | specific heat at constant pressure, Btu per pound per $^{\circ}R$ |
| $c_v$ | specific heat at constant volume, Btu per pound per $^{\circ}R$ |
| $F_n$ | net thrust, pounds |
| f/a | fuel-air ratio |
| $g$ | acceleration of gravity, feet per second per second |
| $\Delta H$ | enthalpy change, Btu per pound |
| $M_0$ | flight Mach number |
| $N$ | engine speed, rpm |
| $P$ | total pressure, pounds per square foot absolute |
| $p$ | static pressure, pounds per square foot absolute |
| $Q$ | heat removed, Btu per hour |
| $R$ | gas constant, foot-pounds per pound per $^{\circ}R$ |
| $T$ | total temperature, $^{\circ}R$ |

$W_a$ mass air flow, pounds per second

$W_f$ mass fuel flow, pounds per hour

$W_g$ mass gas flow, pounds per second

$\beta$ air-bleed ratio, bleed flow/compressor air flow

$\gamma$ ratio of specific heats, $c_p/c_v$

$\delta$ ratio of total pressure to NACA standard sea-level pressure, P/2116

$\theta$ ratio of total temperature to NACA standard sea-level temperature, T/519

Subscripts:

0 free stream

1 diffuser inlet

2 compressor inlet

3 compressor outlet

4 turbine inlet

5 turbine outlet

6 tail-pipe nozzle

c compressor

r rated

t turbine

## ENGINE COMPONENT CHARACTERISTICS

The first step in the analysis is the determination of the performance characteristics of the components of the basic engine, that is, compressor, combustion chamber, and turbine. These characteristics were determined from altitude-wind-tunnel

investigations of a complete axial-flow turbojet engine equipped with tail-pipe nozzles of different sizes in order that an extensive range of operating conditions could be attained for the compressor and the turbine. Inasmuch as a single curve was faired through the data for several ram pressure ratios and altitudes, the Reynolds number effect on the component performance characteristics is not considered in this analysis. Although variations in engine output and economy with Reynolds number would be of the first order, it was considered that these variations with Reynolds number would have only a second-order effect on engine-performance changes due to air bleed. The component characteristics idealized in this manner are shown in figures 1 and 2.

The compressor characteristics are shown in terms of parameters convenient for matching in figure 1. The mass flow through the compressor, which is assumed to be independent of pressure ratio, is given as a function of the engine speed; both factors are corrected to compressor-inlet stagnation conditions. The compressor-power parameter $W_{a,c}\Delta H_c/N\delta_3$ (referred to as torque parameter in reference 1) is plotted as a function of the compressor mass-flow parameter $W_{a,c}N/\delta_3$ for constant values of $N/\sqrt{\theta_3}$. All factors are corrected to compressor-outlet stagnation conditions and are presented as fractions of the rated values at standard sea-level conditions. The data in figure 1 uniquely determine all performance characteristics for the compressor.

Turbine characteristics (fig. 2) are likewise presented in terms of parameters useful for matching, as idealized from the experimental data. The pressure ratio across the turbine $P_4/P_5$ is plotted as a function of the temperature ratio across the turbine $T_4/T_5$, and the turbine-power parameter $W_{a,t}\Delta H_t/N\delta_4$ is given as a function of the turbine mass-flow parameter $W_{a,t}N/\delta_4$ for constant values of $N/\sqrt{\theta_4}$. These characteristics are given as fractions of the values obtained when the engine is operating at rated standard sea-level condition.

Although the component characteristics used in developing the analysis are applicable only to axial-flow engines, the method of analysis is applicable to any turbojet engine, either centrifugal or axial-flow type, in any range of pressure ratios and temperatures.

## BASIC ENGINE PERFORMANCE

Matching procedure. - A basic turbojet engine consists of a compressor, a combustion chamber, and a turbine operating together in such a manner that the rotative speed of the compressor equals the rotative speed of the turbine and that the enthalpy change across the compressor plus the power lost due to friction and heat transfer is equal to the enthalpy change across the turbine. If the work obtained from the fuel mass as it passes through the turbine is assumed equal to the power lost in friction and heat transfer, then

$$W_{a,c}\Delta H_c = W_{a,t}\Delta H_t$$

In addition, the mass flows are related as follows:

$$W_{g,t} = (1+f/a)(1-\beta)W_{a,c}$$

The combustion-chamber pressure drop relates the compressor-outlet conditions to the turbine-inlet conditions.

Compressor and turbine characteristics are plotted as functions of parameters that contain the variables W, $\Delta H$, and N so that the turbine and compressor characteristics can be directly related for the matched condition because of the known relation between compressor and turbine parameters. Thus the compressor characteristics are plotted as functions of $W_{a,c}\Delta H_c/N\delta_3$, $W_{a,c}N/\delta_3$, and $N/\sqrt{\theta_3}$ in figure 1; the turbine characteristics are plotted as functions of $W_{a,t}\Delta H_t/N\delta_4$, $W_{a,t}N/\delta_4$, and $N/\sqrt{\theta_4}$ in figure 2. The compressor parameters $W_{a,c}\Delta H_c/N\delta_3$ and $W_{a,c}N/\delta_3$ can be converted to $W_{a,c}\Delta H_c/N\delta_4$ and $W_{a,c}N/\delta_4$ by use of the combustion-chamber pressure drop. Then the compressor parameters $W_{a,c}\Delta H_c/N\delta_4$ and $W_{a,c}N/\delta_4$ are exactly equal to the turbine parameters $W_{a,t}\Delta H_t/N\delta_4$ and $W_{a,t}N/\delta_4$ when no air is bled from the compressor, inasmuch as $W_{a,c}\Delta H_c$, $W_{a,c}$, and N for the compressor are equal to $W_{a,t}\Delta H_t$, $W_{a,t}$, and N for the turbine. Both the compressor and turbine characteristics can therefore be plotted on the same coordinates (fig. 3). Any point on this chart is therefore an operating point of the basic turbojet engine.

If the lines of figure 3 corresponding to operation without air bleed are considered, selection of a particular point on the figure fixes the values of the parameters $N/\sqrt{\theta_3}$, $N/\sqrt{\theta_4}$,

$W_{a,c}\Delta H_c/N\delta_4$, $W_{a,t}\Delta H_t/N\delta_4$, $W_{a,c}N/\delta_4$, and $W_{a,t}N/\delta_4$ necessary for the matched condition. These parameters can be used, together with the component characteristics of figures 1 and 2, to determine the temperature and pressure ratios for the entire engine and for the engine components at any given corrected speed for the case of zero air bleed.

Bleeding air from the compressor outlet alters the procedure only slightly. With air bleed, the engine performance is affected by the decrease in the mass of working fluid in the cycle and by the changed matching conditions of the compressor and the turbine. Changes in the matching of these two components can be allowed for directly on the matching chart (fig. 3). The total work furnished by the turbine minus the losses due to friction and heat transfer must equal the work absorbed by the compressor regardless of the amount of air bleed. Assuming again that the work obtained from the fuel mass in passing through the turbine is equal to the losses,

$$W_{a,c}\Delta H_c = W_{a,t}\Delta H_t$$

The ordinate of figure 3 therefore remains unchanged with air bleed for both the compressor and the turbine. The relation between the mass-flow parameters is changed, however, because $W_{a,t}$ is decreased from $W_{a,c}$ by the amount of air bled off. Consequently for a given percentage air bleed, the turbine-characteristic chart must be shifted to the right to compensate for the lower mass flow. The abscissa of the matching chart therefore has two scales, one for the compressor and one for the turbine, and the lines of constant $N/\sqrt{\theta_4}$ are shifted to the right. The broken lines and the lower abscissa scale in figure 3 illustrate this shift in turbine coordinates for an air bleed of 5 percent of the compressor air flow. The matching procedures with and without air bleed are similar, provided the correct abscissa scales and $N/\sqrt{\theta_4}$ lines are used for the desired air bleedoff.

The determination of a match point and the subsequent calculation of the basic engine performance is accomplished in the following manner: The selection of a point on figure 3 (using an abscissa scale and lines of constant $N/\sqrt{\theta_4}$ corresponding to the desired air bleed) establishes a possible operating condition for the compressor-turbine combination. The values of $N/\sqrt{\theta_3}$ and $N/\sqrt{\theta_4}$ determine the required temperature ratio across the

combustion chamber $T_4/T_3$. The compressor temperature ratio $T_3/T_2$ can be found from the coordinates of the matching chart by means of the relation

$$\frac{T_2}{T_3} = \frac{\theta_2}{\theta_3} = 1 - \frac{\Delta T_c}{519\ \theta_3}$$

$$= 1 - \frac{\Delta H_c}{519\ c_{p,c}\theta_3}$$

where $\Delta H_c/\theta_3$ can be found from $W_{a,c}\Delta H_c/N\delta_3$, $W_{a,c}N/\delta_3$, and $N/\sqrt{\theta_3}$. A value of 0.24 Btu per pound per $^{o}R$ was assumed for the specific heat $c_{p,c}$. The turbine temperature ratio can be found in a similar manner by use of the relation

$$\frac{T_5}{T_4} = \frac{\theta_5}{\theta_4} = 1 - \frac{\Delta T_t}{519\ \theta_4}$$

$$= 1 - \frac{\Delta H_t}{519\ c_{p,t}\theta_4}$$

A value of 0.27 Btu per pound per $^{o}R$ was assumed for $c_{p,t}$. The over-all engine temperature ratio $T_5/T_2$ is then uniquely fixed for any point on the matching chart, inasmuch as it is the product of the three known temperature ratios $T_3/T_2$, $T_4/T_3$, and $T_5/T_4$.

The pressure ratio across the compressor can be determined from

$$\frac{P_3}{P_2} = \frac{W_{a,c}\sqrt{\theta_2}/\delta_2}{W_{a,c}\sqrt{\theta_3}/\delta_3}\sqrt{\frac{T_3}{T_2}}$$

where the compressor air flow corrected to compressor-inlet conditions $W_{a,c}\sqrt{\theta_2}/\delta_2$ is found from figure 1 using $N/\sqrt{\theta_2}$ determined from $N/\sqrt{\theta_3}$ and $T_3/T_2$. The compressor air flow corrected to compressor-outlet conditions $W_{a,c}\sqrt{\theta_3}/\delta_3$ is obtained in the following manner:

$$\frac{W_{a,c}\sqrt{\theta_3}}{\delta_3} = \frac{W_{a,c}N/\delta_4}{N/\sqrt{\theta_3}} \frac{P_4}{P_3}$$

where $\frac{W_{a,c}N/\delta_4}{N/\sqrt{\theta_3}}$ is found from the matching chart (fig. 3) and the combustion-chamber pressure ratio $P_4/P_3$ is assumed equal to 0.945.

The over-all engine pressure ratio is then the product of $P_3/P_2$, $P_4/P_3$, and $P_5/P_4$.

Over-all pumping characteristics. - In presenting the performance of the basic turbojet engine, the method of reference 2 is used. The compressor, the combustion chamber, and the turbine are considered a basic turbojet engine or pump, the purpose of which is to increase the temperature and the pressure of the working fluid passing through it. The pumping characteristics consist of a curve of over-all engine pressure ratio as a function of over-all engine temperature ratio for constant values of engine speed and air bleed and of a curve of engine-inlet mass flow (identical with compressor-inlet mass flow) as a function of engine speed. The variation of engine pressure ratio with engine temperature ratio is plotted in figure 4 for air bleeds of 0, 5, 10, and 15 percent of the compressor air flow and for corrected engine speeds $N/\sqrt{\theta_2}$ of 0.9, 1.0, and 1.1 times the rated values for sea-level static operation. The air mass flow - engine speed characteristics are given in figure 1.

In addition to the over-all engine pressure and temperature ratios, it may be desirable to know the turbine-inlet temperature ratio $T_4/T_2$ in order to determine the maximum cycle temperatures. The turbine-inlet temperature ratio as a function of the over-all engine temperature ratio is presented in figure 5 for air bleeds of 0 to 15 percent of the compressor air flow and for corrected engine speeds $N/\sqrt{\theta_2}$ of 0.9, 1.0, and 1.1 times the rated value for sea-level static operation. For the same range of air bleeds and engine speeds, the compressor temperature and pressure ratios are presented as functions of the over-all engine temperature ratio in figures 6 and 7, respectively.

## PROPULSION-SYSTEM PERFORMANCE

Determination of propulsion parameters. - The propulsion system is the basic turbojet engine combined with an inlet system and a tail-pipe nozzle. Performance characteristics of the basic turbojet engine are obtained by the methods of the preceding analysis.

Engine-inlet characteristics are generally presented as functions of flight Mach number in terms of a pressure ratio, such as the inlet pressure ratio $P_2/p_0$. The following values of $P_2/p_0$ (defined herein as ram pressure ratio) were used: for static engine-inlet conditions

$$\frac{P_2}{p_0} = 0.99$$

and for flight conditions

$$\frac{P_2}{p_0} = 1 + 0.92\,\frac{P_1 - p_0}{p_0}$$

Tail-pipe-nozzle characteristics were calculated as functions of over-all engine pressure and temperature ratios, engine-inlet pressure ratio, mass flow of gas leaving the engine, and nozzle area by use of one-dimensional flow relations and the equation of continuity. The equations expressing the nozzle characteristics in a form convenient for the matching of the basic engine and the tail-pipe nozzle are, for the unchoked condition,

$$\frac{T_5}{T_2'} = \frac{\dfrac{2\gamma g(2116)^2}{519\,R(\gamma-1)}\left[\left(\dfrac{P_5}{P_2}\dfrac{P_2}{p_0}\right)^{\frac{2(\gamma-1)}{\gamma}} - \left(\dfrac{P_5}{P_2}\dfrac{P_2}{p_0}\right)^{\frac{\gamma-1}{\gamma}}\right]}{\left(\dfrac{W_g\sqrt{\theta_2}}{C_d A_6 \delta_2}\dfrac{P_2}{p_0}\right)^2}$$

and for the choked convergent nozzle,

$$\frac{T_5}{T_2} = \left[\frac{\gamma g (2116)^2}{519\ R\left(\frac{\gamma+1}{2}\right)^{\frac{\gamma+1}{\gamma-1}}}\right] \frac{\left(\frac{P_5}{P_2}\right)^2}{\left(\frac{W_g\sqrt{\theta_2}}{C_d A_6 \delta_2}\right)^2}$$

The nozzle characteristics from these equations are plotted in figure 8 for various values of $W_{g,t}\sqrt{\theta_2}/C_d A_6 \delta_2$ for a ram pressure ratio of 1.35.

The process of matching the nozzle characteristics that incorporate the ram pressure ratio with the basic engine characteristics determines the propulsion-system performance. For the matched condition, the mass flows through the components are related as

$$\frac{W_{g,t}\sqrt{\theta_2}}{C_d A_6 \delta_2} = \frac{W_{a,c}\sqrt{\theta_2}}{C_d A_6 \delta_2} (1-\beta)\left(1 + \frac{f}{a}\right)$$

where $W_{g,t}$ is the tail-pipe mass flow as well as the turbine mass flow. The corrected compressor air flow $W_{a,c}\sqrt{\theta_2}/\delta_2$ can be found from figure 1 for any given corrected engine speed. Values are assumed for $f/a$, and $C_d$ was assumed to be 0.98, so that the corrected gas flow $W_{g,t}\sqrt{\theta_2}/C_d A_6 \delta_2$ can be calculated for a given tail-pipe area $A_6$. These conditions then establish a definite line on the nozzle curves, which is plotted across the engine line for the same speed on the $P_5/P_2$ - $T_5/T_2$ plane (fig. 9). The intersection of these lines gives the values of $P_5/P_2$ and $T_5/T_2$ consistent with the assumed fuel-air ratio. The calculation may be refined at this point by finding the turbine-inlet temperature ratio $T_4/T_2$ from figure 5 and the compressor temperature ratio $T_3/T_2$ from figure 6; these ratios together with a value of $T_2$ from the flight conditions may be used to determine the combustion temperature rise so that the method of reference 3 can be used to find $f/a$. In this calculation, the heating value of the fuel was assumed to be 18,700 Btu per pound and the combustion efficiency to be 0.95. With this new $f/a$, a new nozzle line can be drawn across the engine line to determine more accurately the operating point of the propulsion system. When the value of $T_5/T_2$ is established in this manner, the turbine-inlet temperature and the compressor temperature and pressure ratios can be determined for

the propulsion system by use of figures 5 and 7, respectively. The corrected net thrust can be calculated by use of the following equations, which contain the known quantities $P_5/P_2$, $P_2/p_0$, $T_5/T_2$, $W_{a,c}\sqrt{\theta_2}/\delta_2$, f/a, and the flight Mach number $M_0$: for the unchoked nozzle,

$$\frac{F_n}{\delta_2} = \left\{ \left(1 + \frac{f}{a}\right) \left[ \sqrt{\frac{2\gamma R\ 519}{g(\gamma-1)}} \sqrt{\frac{T_5}{T_2}} \sqrt{1 - \left(\frac{P_2}{P_5}\frac{p_0}{P_2}\right)^{\frac{\gamma-1}{\gamma}}} \right] - \sqrt{\frac{519\ \gamma R}{g}} \frac{M_0}{\sqrt{1 + \frac{\gamma-1}{2} M_0^2}} \right\} \frac{W_{a,c}\sqrt{\theta_2}}{\delta_2}$$

or, for the choked convergent nozzle,

$$\frac{F_n}{\delta_2} = \left\{ \left(1 + \frac{f}{a}\right) \sqrt{\frac{519\ R}{\gamma g} \left(\frac{\gamma+1}{2}\right)^{\frac{\gamma+1}{\gamma-1}}} \sqrt{\frac{T_5}{T_2}} \left[ \frac{2}{\left(\frac{\gamma+1}{2}\right)^{\frac{1}{\gamma-1}}} - \frac{P_2}{P_5}\frac{p_0}{P_2} \right] - \sqrt{\frac{519\ \gamma R}{g}} \frac{M_0}{\sqrt{1 + \frac{\gamma-1}{2} M_0^2}} \right\} \frac{W_{a,c}\sqrt{\theta_2}}{\delta_2}$$

The specific fuel consumption is found by means of the expression

$$\frac{W_f}{F_n\sqrt{\theta_2}} = \frac{\frac{f}{a}\left(\frac{W_{a,c}\sqrt{\theta_2}}{\delta_2}\right)(1-\beta)\ 3600}{\theta_2\ F_n/\delta_2}$$

Presentation of performance parameters. - The propulsion-system performance for different operating conditions is presented in the form of working charts in figures 10 to 15.

1230

Performance data for operation with a variable-area tail-pipe nozzle at a ram pressure ratio $P_2/p_0$ of 1.35 are given in figures 10 to 12. Parts (a), (b), and (c) of each figure represent corrected engine speeds of 0.9, 1.0, and 1.1 times the rated value, respectively. The net thrust is used as a parameter in all figures. In figure 10 the turbine-inlet temperature ratio and the tail-pipe-nozzle area are plotted as functions of the air-bleed ratio. Lines of constant power-removal factor $\frac{Q/\delta_2\sqrt{\theta_2}}{(F_n/\delta_2)_r}$ (Btu/lb rated thrust) are shown on the temperature ratio - air bleed chart to permit entry into the charts if the heat requirement and either the turbine-inlet temperature ratio or the required thrust are known. The values of the power-removal factor shown are for a rated compressor pressure ratio of 4.0. For higher rated compressor pressure ratios, the power-removal factor should be increased by 0.8 of the percentage increase in the pressure ratio. The power removed from the engine is defined as the work done during compression on the air that is bled off. When the percentage of air bleed is determined from figure 10, the remaining performance parameters can be determined from figures 11 and 12. The thrust specific fuel consumption and the equivalent power-removal specific fuel consumption are given in figure 11. The values of the equivalent power-removal specific fuel consumption shown are for a rated compressor pressure ratio of 4.0. For higher rated compressor pressure ratios, the equivalent power-removal specific fuel consumption should be decreased by 0.8 of the percentage increase in the pressure ratio. In the determination of $\Delta W_f/Q$ the entire increase in fuel consumption accompanying air bleed (due to the mismatching of the engine components and to the removal of more work per unit of mass flow through the turbine) was charged to the work in compressing the air that was bled off. The state of the air bled from the engine is available from the compressor temperature and pressure ratios given in figure 12.

Figures 10 to 12 are calculated for a ram pressure ratio of 1.35. If a range of ram pressure ratios from 1.2 to 1.6 is considered, however, the values of each of the performance parameters shown in figures 10 to 12 are always within 3 percent of their values for the ram pressure ratio of 1.35. Consequently, the curves in these figures can be used with adequate accuracy for flight conditions within the range of ram pressure ratios from 1.2 to 1.6. For static engine-inlet conditions, however, another set of curves is required. Figures 13 to 15 are similar to figures 10 to 12, but represent static inlet conditions. These data show the same general trend as for the higher ram pressure ratio (1.35) and are applied in the same manner.

An example illustrating the use of the charts in the evaluation of turbojet-engine performance with air bleed is presented in the appendix.



## LIMITATIONS OF ANALYSIS

Inasmuch as the analysis presented herein is based on the component characteristics of a particular engine, the accuracy of performance prediction for any given engine would depend on the degree of similarity between component characteristics for the engine in question and for the engine used in this analysis. If the components of an engine have characteristics similar to those shown in figures 1 and 2, the relation between engine temperature ratio and engine pressure ratio as a function of air bleed will closely approximate the data of figure 4.

In the computation of performance data from the operating points determined by the intersection of nozzle and engine pumping characteristics, certain precautions must be observed. The angle between the nozzle and engine curves is small, and small displacements of either set of curves for any reason will therefore cause large shifts in the operating point and consequently in the engine over-all pressure and temperature ratios. This statement is clearly illustrated in figure 16. The solid lines represent the nozzle and engine characteristics with no air bleed and for 10-percent air bleed, assuming no change in nozzle area or compressor mass flow. The dashed lines show these curves for 10-percent air bleed if the compressor mass flow were increased 1 percent by bleeding air. The operating point for 10-percent air bleed has moved so that the accompanying increase in engine temperature ratio has changed from 3.0 to 8.6 percent. Slight discrepancies in fairing either the nozzle or engine curves will have a similar effect.

From the foregoing discussion, it follows that in order for the constant-area operation of two engines to agree, the pumping characteristics must agree almost perfectly. It therefore cannot be expected that perfect agreement in operating characteristics between two engines with air bleed at constant area will exist. If a given temperature requirement with air bleed is used (such as constant turbine-outlet temperature), however, the agreement in performance between two engines should be as good as the agreement in pumping characteristics if the level of operation (magnitude of compressor pressure ratio and turbine-inlet temperature) of each engine is taken into account. Agreement in the over-all pumping characteristics does not necessarily mean that the propulsive-system performance

will agree as well, because percentage changes in propulsive characteristics also depend on the level of operation, that is, the actual engine temperatures and pressure ratios. Most current turbojet engines, however, operate in the same range of temperatures and pressure ratios. Consequently, the propulsive characteristics of these engines with air bleed can be determined with reasonable accuracy from figures 10 to 15. If turbine-inlet temperatures are appreciably higher than 2000° R, or if compressor pressure ratios above 4 or 5 are used, propulsion characteristics could be more accurately determined directly from calculations based on figures 4 to 7 if the component characteristics are similar. Even though the component characteristics of an engine are different from those used in the present analysis, and the charts presented herein are consequently not applicable, the performance of the engine with air bleed can be determined by applying the analytical method developed herein.

## APPLICATIONS OF ANALYSIS

Many problems involving the bleeding of air from the compressor outlet of a turbojet engine can be solved by the use of the charts presented. Although the performance calculations are beyond the intended scope of this report, consideration must be given to several factors in the application of the analytical results to any specific problem. Because the working charts are presented for corrected engine speeds of 0.9, 1.0, and 1.1 of rated value, interpolation must be used in determining the engine performance at intermediate speeds. Although linear interpolation may be used with fair accuracy, greater accuracy can be obtained by using curves that have been faired through the values of the engine parameters for the three speeds.

The state of the air available for auxiliary use will usually differ from the state of the air leaving the compressor (figs. 6, 7, 12, and 15) because of throttling and heat-transfer losses that are not considered in this analysis. Considerable losses may be involved, the magnitudes of which will depend on the design of the bleed system and on the quantity of air bled off.

In the application of compressor air bleed to anti-icing problems (or other problems where the air bled off is used as a heat source), the energy available for the desired use may differ from the values shown in figures 10 and 13. The values of the power-removal factor shown are for a rated compressor pressure ratio of 4.0. For different values of rated compressor pressure

ratio, the values from figures 10 and 13 should be corrected as previously stated. The power-removal factor represents the energy available from the bleed air if the temperature is lowered to the compressor-inlet total temperature. If the conditions of the problem indicate that the temperature to which the bleed air can be lowered is different from the compressor-inlet temperature, a utilization factor must be used in determining the power required from the engine.

## COMPARISON OF EXPERIMENTAL AIR-BLEED DATA WITH ANALYTICAL VALUES

A comparison between the results of the present analysis and experimental results of an air-bleed investigation is presented in figures 17 and 18. The experimental data were obtained from an altitude-wind-tunnel investigation of an axial-flow-type turbojet engine with approximately 25-percent higher rated compressor pressure ratio and 10-percent higher rated turbine-inlet temperature than the engine used as the basis for the analysis. Experimental bleed data for 91 and 103 percent of rated corrected engine speed at a ram pressure ratio of 1.2 were obtained for various exhaust-nozzle areas and air bleeds from 0 to 11 percent. The analytical and experimental results of bleeding air from the compressor outlet at constant corrected engine speed and constant turbine-outlet temperature are presented in figure 17. The analytical performance was calculated from the working charts (figs. 10 and 11) for a ram pressure ratio of 1.35. An excellent check is obtained between the analytical and experimental changes in engine pressure ratio, thrust, and specific fuel consumption. The slight discrepancies between the analytical and experimental changes in engine pressure ratio are due to differences in the basic characteristics of the two engines. Discrepancies between the analytical and experimental changes in thrust and specific fuel consumption are due to a combination of differences in basic engine characteristics, flight conditions, and level of operation.

Comparison of figures 17(a) and 17(b) shows that engine speed had little effect on the percentage changes of engine pressure ratio, thrust, and specific fuel consumption. Constant-area performance with air bleed can therefore be predicted if the turbine-outlet temperature is held constant, inasmuch as the variation of engine speed for this mode of operation is slight.

The accurate prediction of constant-area constant-speed air-bleed performance is much more difficult, because even slight discrepancies in the pumping characteristics will cause large differences in the engine temperature and pressure ratios. This effect is due to the slight angle of intersection between the pumping and nozzle characteristics, as previously pointed out. A comparison between the analytical and experimental changes in engine temperature and pressure ratios for constant-speed, constant-area operation is presented in figure 18. The discrepancies between the analytical and experimental changes in engine temperature and pressure ratios are large. A fair check on thrust and specific fuel consumption is obtained, however, for values of $\beta$ up to 0.06 or 0.08.

## CONCLUDING REMARKS

The performance of an axial-flow-type turbojet engine with compressor-outlet air bleed can be determined by the method presented herein. The results of this analysis are presented in terms of generalized performance charts that are applicable to a wide range of operating conditions. Propulsion characteristics with air bleed for engines with similar component characteristics and with pressure ratios in the range of 4 to 5 and turbine-inlet temperatures of approximately 2000° R can be determined by the use of these performance charts. The method of the analysis, however, is applicable for any turbojet engine, with a centrifugal or axial-flow compressor, in any range of compressor pressure ratio and turbine-inlet temperature.

An excellent check is obtained between analytical and experimental air-bleed performance at constant tail-pipe temperatures. Because of the high degree of sensitivity of the engines to tail-pipe-nozzle area, however, the prediction of constant-area, constant-speed air-bleed performance is less accurate.

Lewis Flight Propulsion Laboratory,
National Advisory Committee for Aeronautics,
Cleveland, Ohio, September 12, 1949.

## APPENDIX - USE OF PERFORMANCE CHARTS

The use of the performance charts presented in figures 9 to 14 in solving performance problems involving air bleed is illustrated by the following example. A hypothetical engine, which is similar to existing engines, has the following characteristics at normal sea-level rated operation:

| | |
|---|---|
| $F_n/\delta_2$, lb | 4000 |
| $N/\sqrt{\theta_2}$, rpm | 10,000 |
| $T_4$, °R | 1870 |
| $W_f/F_n\sqrt{\theta_2}$, lb/(hr)(lb thrust) | 1.0 |
| $A_6$, sq ft | 1.215 |
| $P_3/P_2$ | 4.0 |
| $T_3/T_2$ | 1.57 |

The engine has a variable-area tail-pipe nozzle and is operating at rated corrected engine speed. At an altitude of 20,000 feet and a flight Mach number of 0.7, a corrected net thrust $F_n/\delta_2$ of 2000 pounds is required from the engine. The airplane requires 500,000 Btu per hour to be delivered from the compressor outlet by bleeding air.

From the flight conditions and the inlet characteristics, the following values are obtained:

| | |
|---|---|
| $P_2/p_0$ | 1.352 |
| $P_2$, lb/sq ft absolute | 1315 |
| $T_2$, °R | 492 |
| $\delta_2$ | 0.623 |
| $\theta_2$ | .948 |

Inasmuch as the ram pressure ratio falls within the range of 1.2 to 1.6, figures 10 to 12 are applicable. Because the engine is operating at rated corrected speed, parts (b) of these figures should be used.

In order to enter the figures, it is necessary to evaluate the thrust parameter $\frac{F_n/\delta_2}{(F_n/\delta_2)_r}$ and the power-removal factor $\frac{Q/\delta_2\sqrt{\theta_2}}{(F_n/\delta_2)_r}$

The first parameter is simply the required corrected net thrust of 2000 divided by 4000, or 0.5. The power-removal factor is evaluated as

$$\frac{Q/\delta_2\sqrt{\theta_2}}{(F_n/\delta_2)_r} = \frac{500{,}000/0.623\sqrt{0.948}}{4000}$$

$$= 206$$

Then the air bleed required (fig. 10(b)) is 5.18 percent of the compressor air flow. The remaining peformance parameters are obtained from figures 10 to 12 with the air bleed and $\frac{F_n/\delta_2}{(F_n/\delta_2)_r}$ known. The results are presented in fractional and absolute form in the following table; the absolute values are found by applying the appropriate rated sea-level engine-performance parameters and values of $P_2$, $T_2$, $\delta_2$, and $\theta_2$, obtainable from reference 4, to the fractional values read from the figures:

| | |
|---|---|
| $\frac{T_4/T_2}{(T_4/T_2)_r}$ | 0.849 |
| $T_4$, °R | 1505 |
| $A_6/(A_6)_r$ | 1.08 |
| $A_6$, sq ft | 1.31 |
| $\frac{W_f/F_n}{(W_f/F_n)_r}$ | 1.403 |
| $W_f/F_n$ lb/(hr)(lb thrust) | 1.368 |
| $\Delta W_f/Q$, lb/Btu | $3.94 \times 10^{-4}$ |
| $\frac{P_3/P_2}{(P_3/P_2)_r}$ | 0.855 |
| $P_3/P_2$ | 3.42 |
| $\frac{T_3/T_2}{(T_3/T_2)_r}$ | 0.958 |
| $T_3$, °R | 740 |

## REFERENCES

1. Goldstein, Arthur W.: Analysis of Performance of Jet Engine from Characteristics of Components. I - Aerodynamic and Matching Characteristics of Turbine Component Determined with Cold Air. NACA Rep. 878, 1947.

2. Sanders, Newell D., and Behun, Michael: Generalization of Turbojet-Engine Performance in Terms of Pumping Characteristics. NACA TN 1927, 1949.

3. Turner, L. Richard, and Lord, Albert M.: Thermodynamic Charts for the Computation of Combustion and Mixture Temperatures at Constant Pressure. NACA TN 1086, 1946.

4. The Staff of the Ames 1- by 3-Foot Supersonic Wind-Tunnel Section: Notes and Tables for use in the Analysis of Supersonic Flow. NACA TN 1428, 1947.

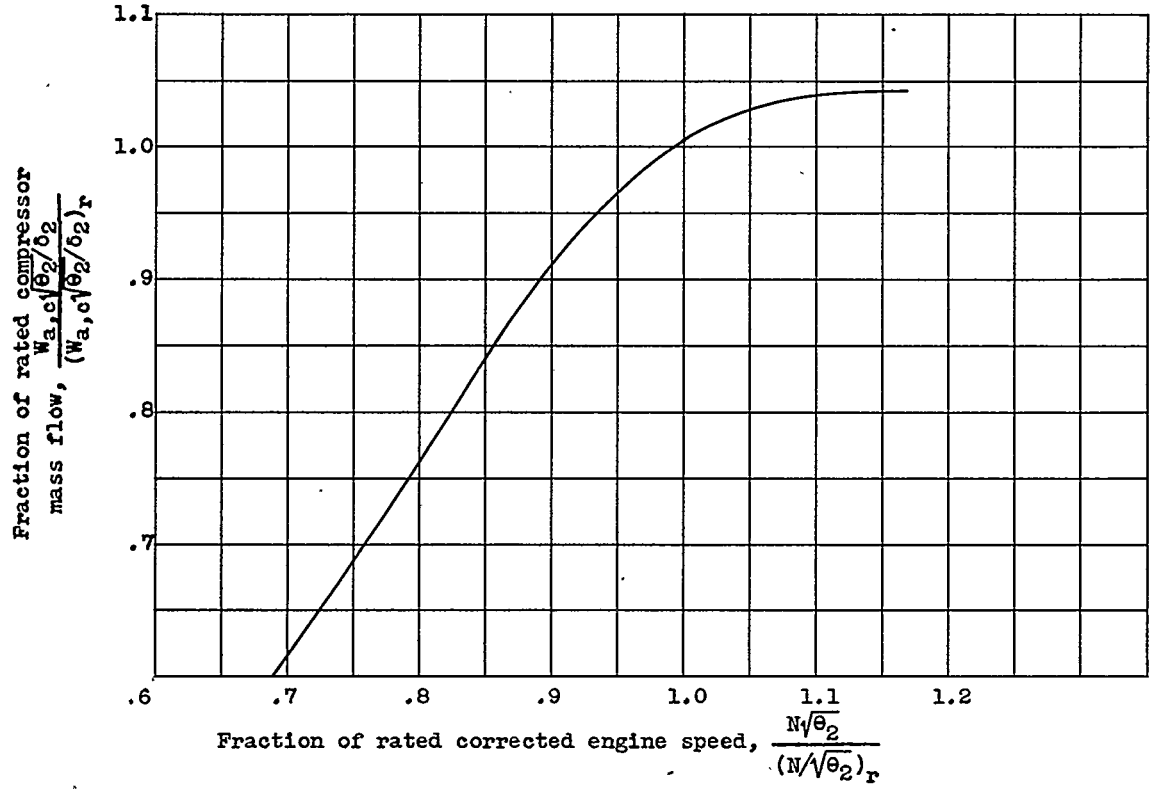


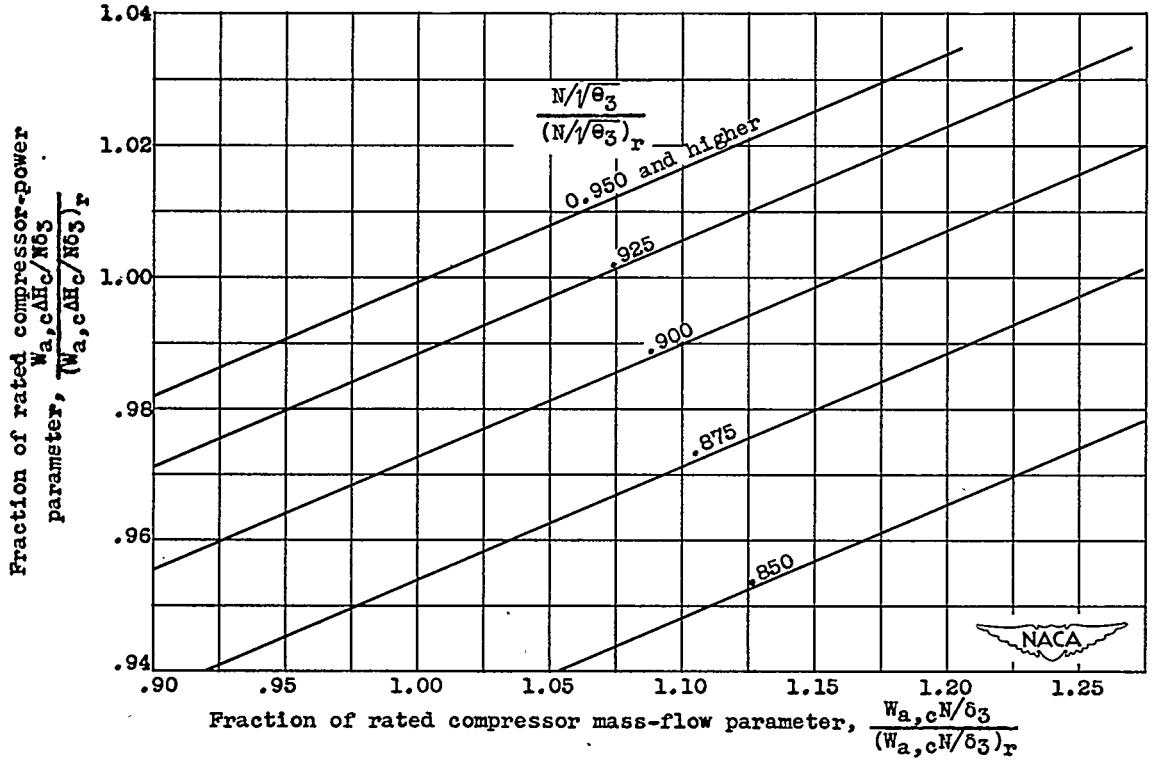


Figure 1. - Idealized axial-flow-compressor characteristics.

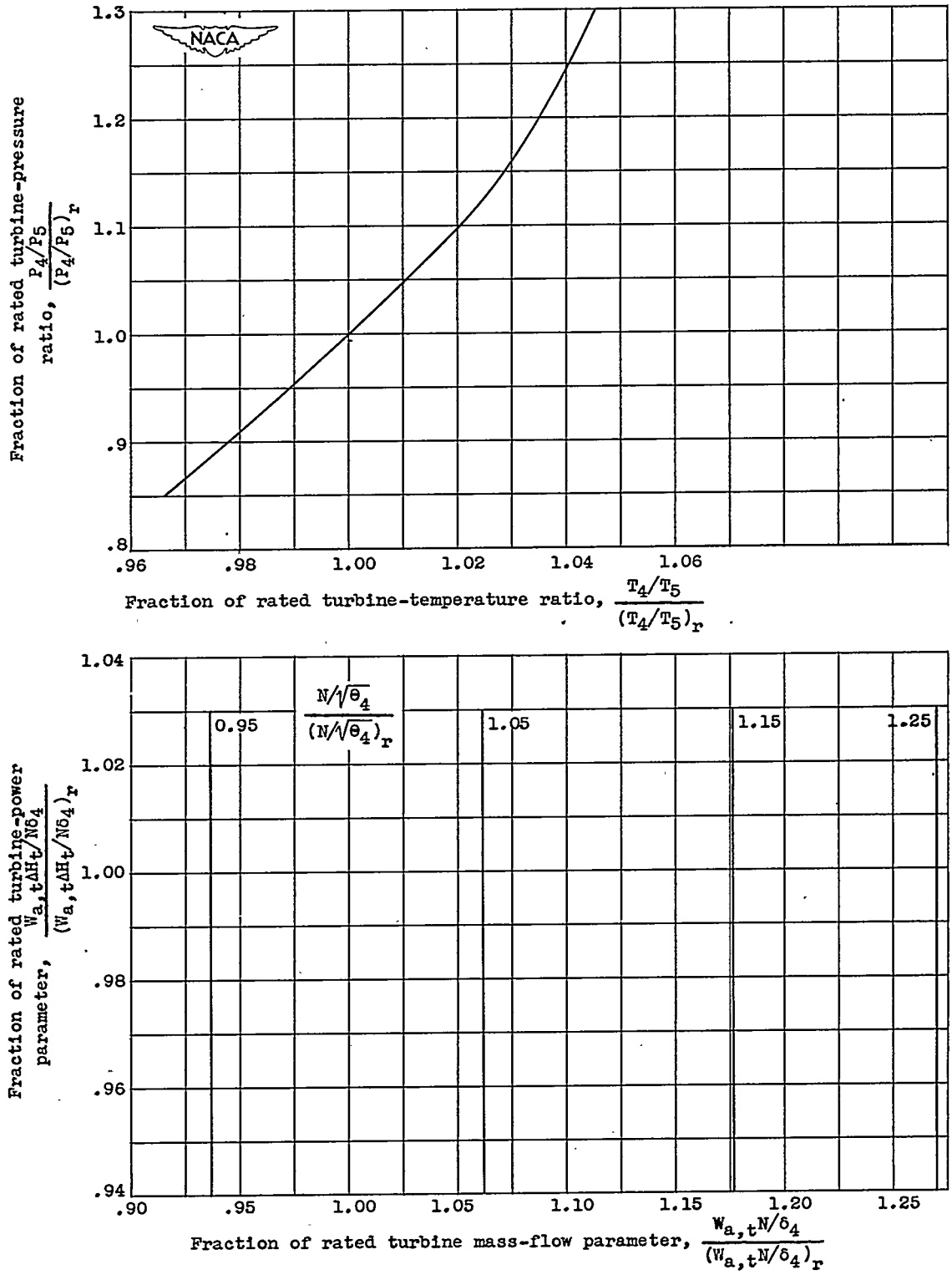


Figure 2. - Idealized turbine characteristics.

1230

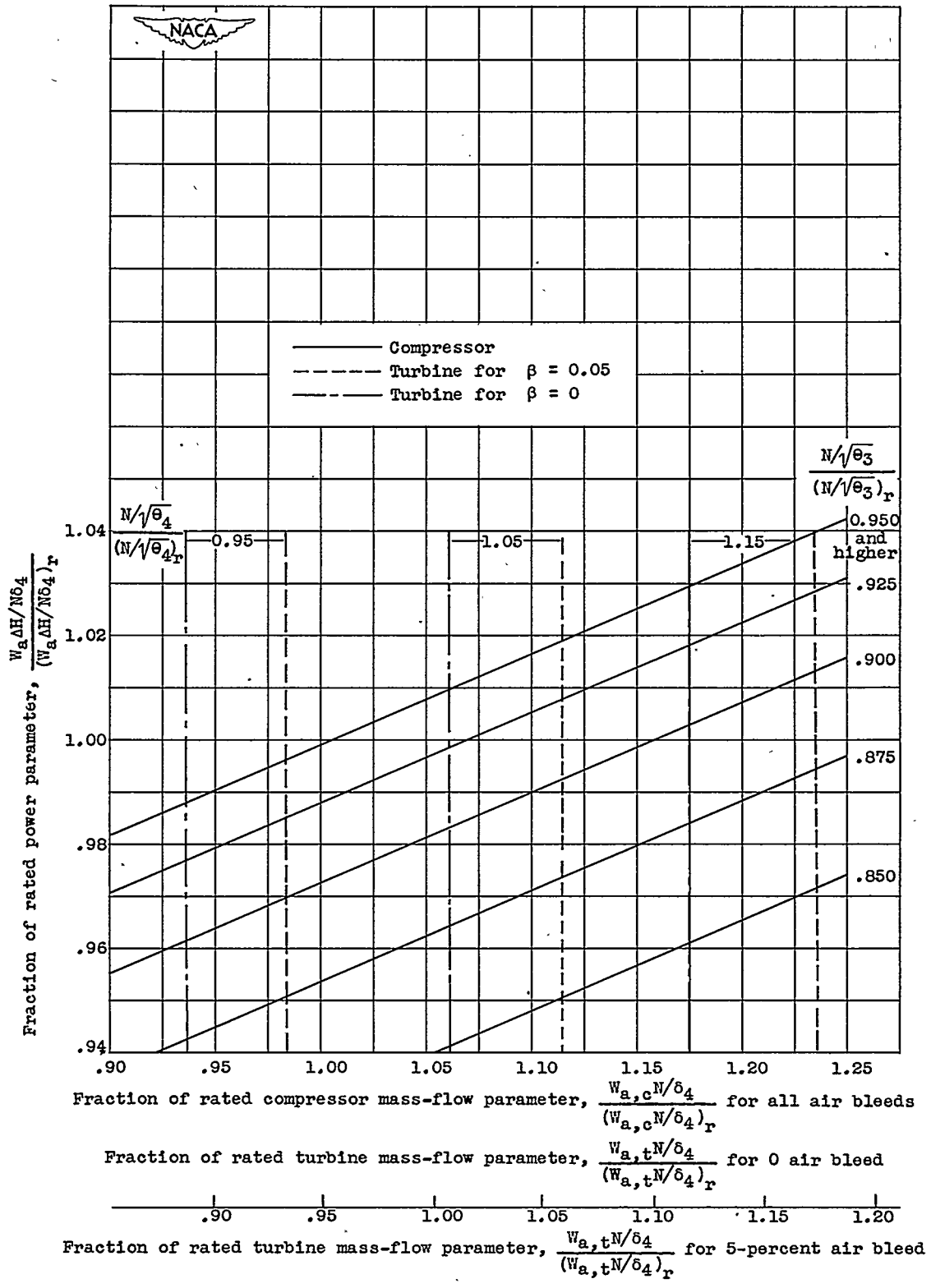


Figure 3. - Compressor and turbine matching chart for air-bleed ratios β of 0 and 0.05.

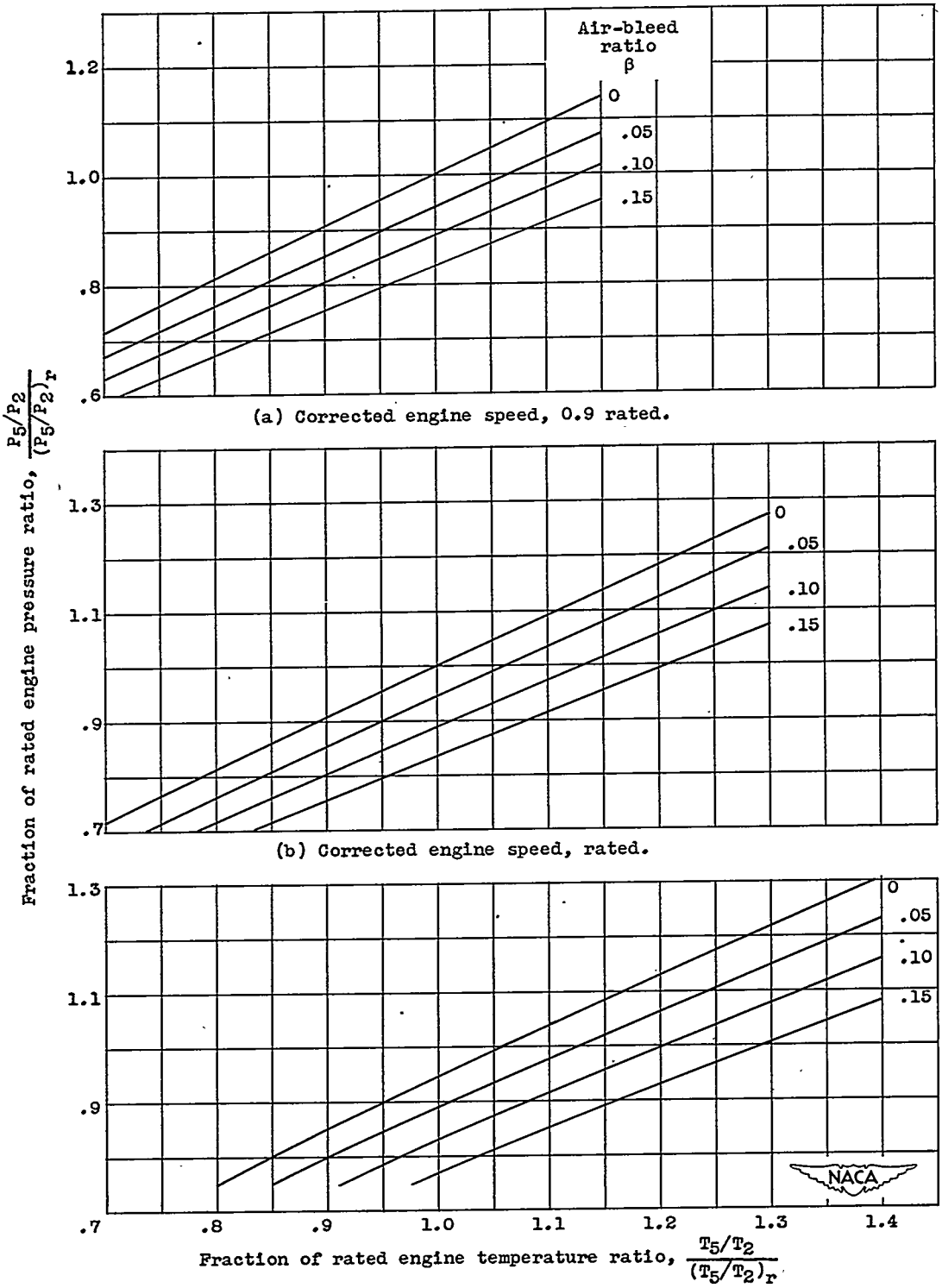


(a) Corrected engine speed, 0.9 rated.

(b) Corrected engine speed, rated.

(c) Corrected engine speed, 1.1 rated.

Figure 4. - Variation of engine pressure ratio with engine temperature ratio and air bleed for three engine speeds.

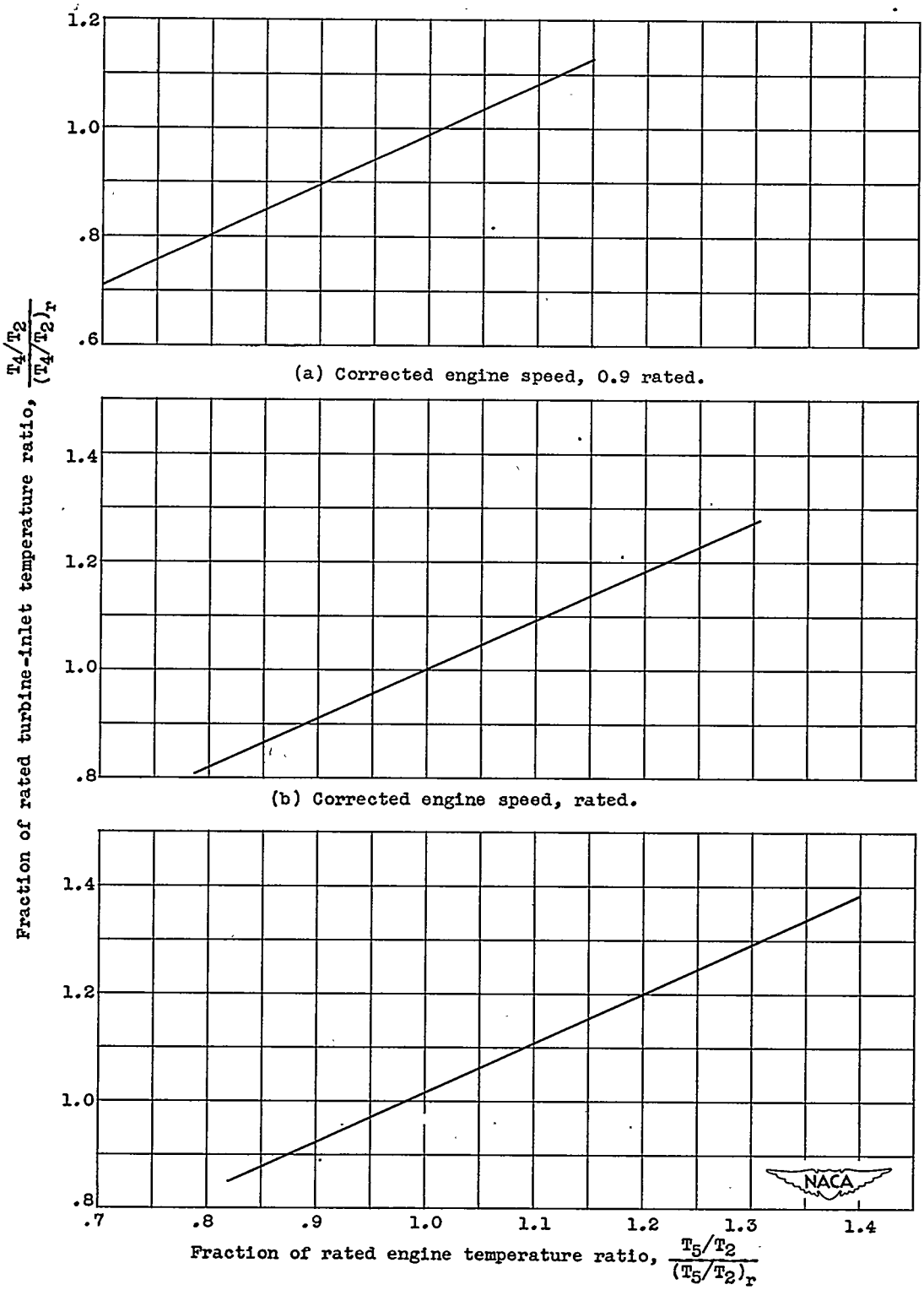


(a) Corrected engine speed, 0.9 rated.

(b) Corrected engine speed, rated.

(c) Corrected engine speed, 1.1 rated.

Figure 5. - Variation of turbine-inlet temperature ratio with engine temperature ratio for three engine speeds and air-bleed ratios of 0 to 0.15.

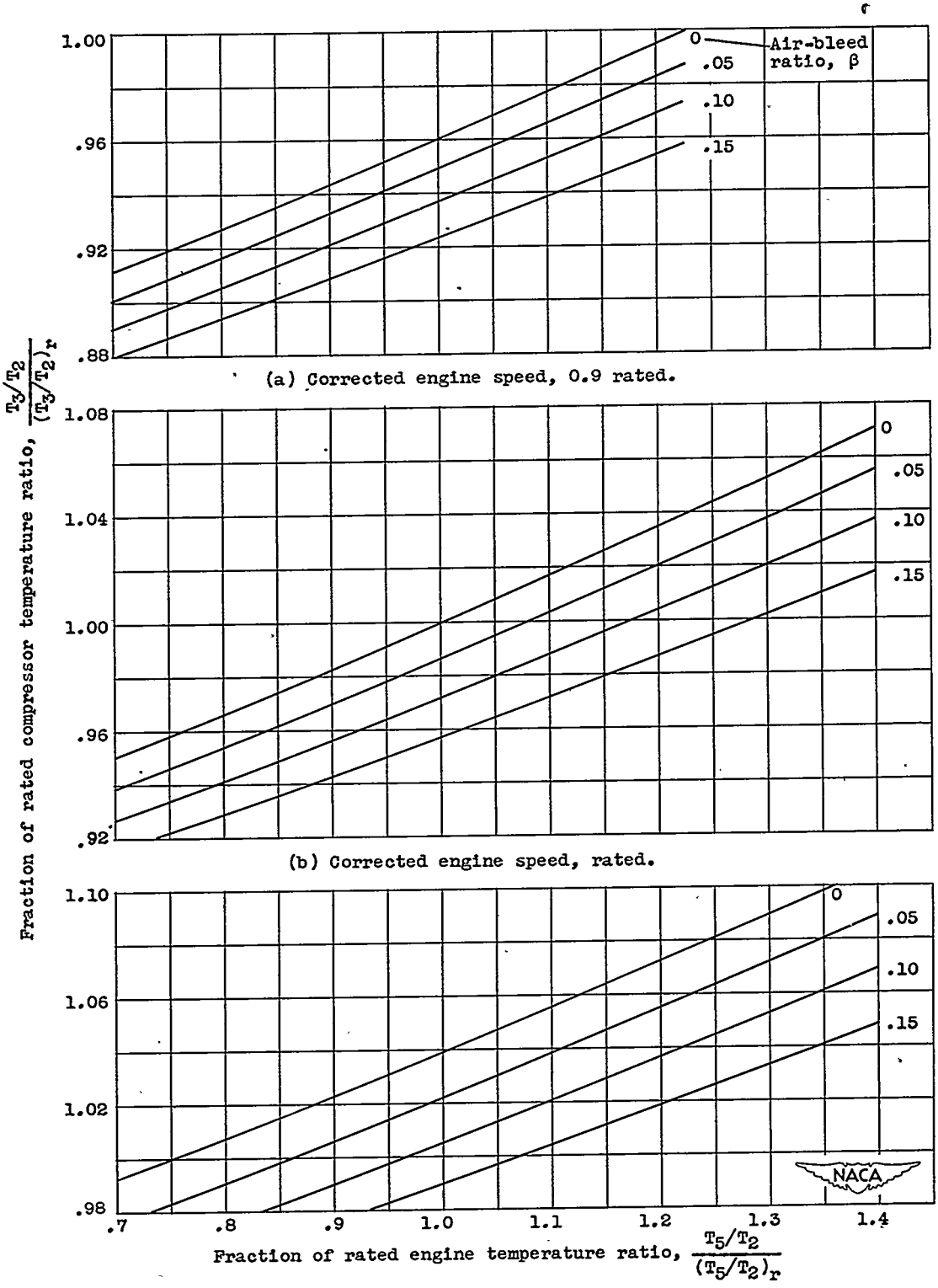


(a) Corrected engine speed, 0.9 rated.

(b) Corrected engine speed, rated.

(c) Corrected engine speed, 1.1 rated.

Figure 6. - Variation of compressor temperature ratio with engine temperature ratio and air bleed for three engine speeds.

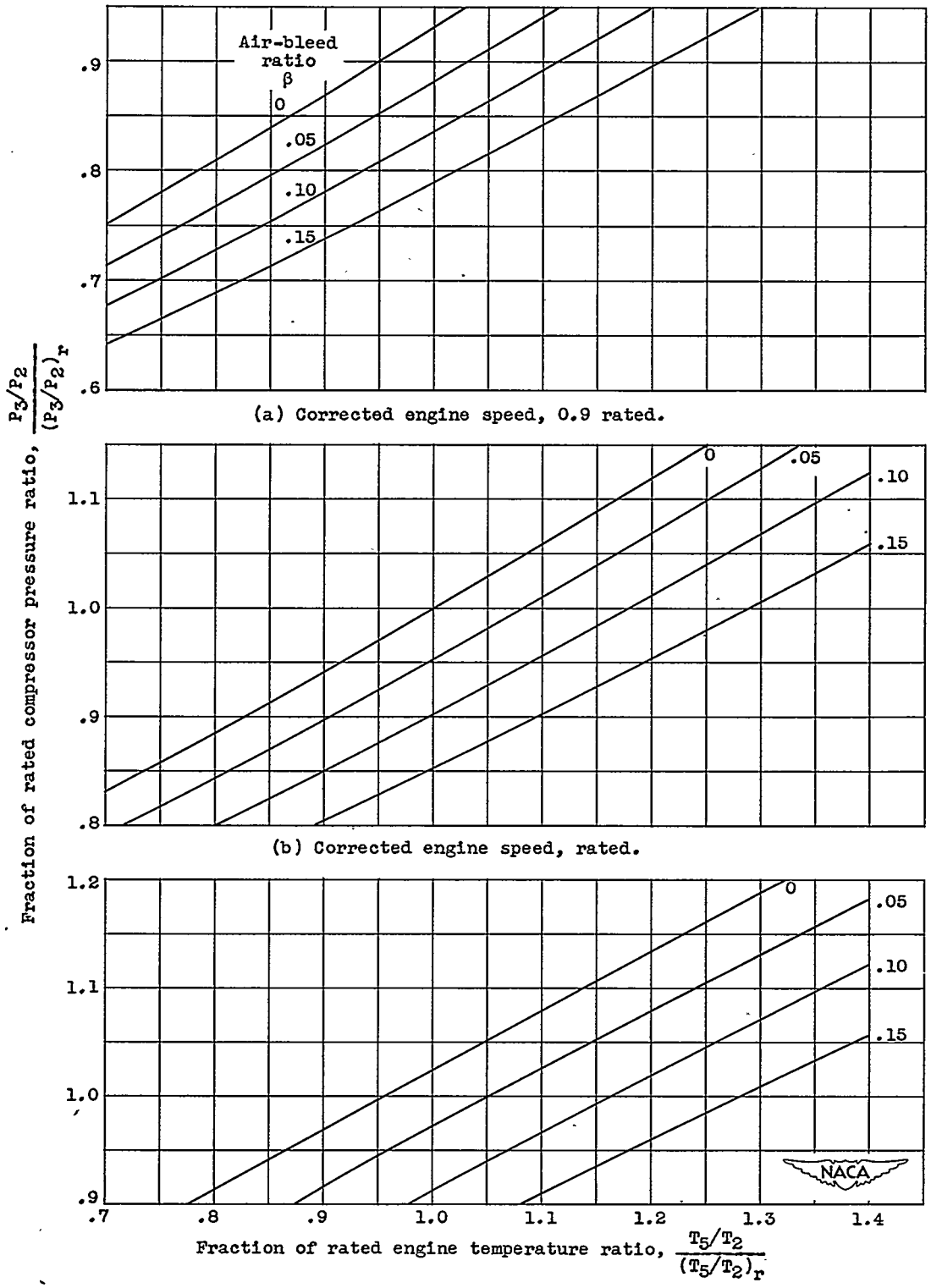


Figure 7. Variation of compressor pressure ratio with engine temperature ratio and air bleed for three engine speeds.

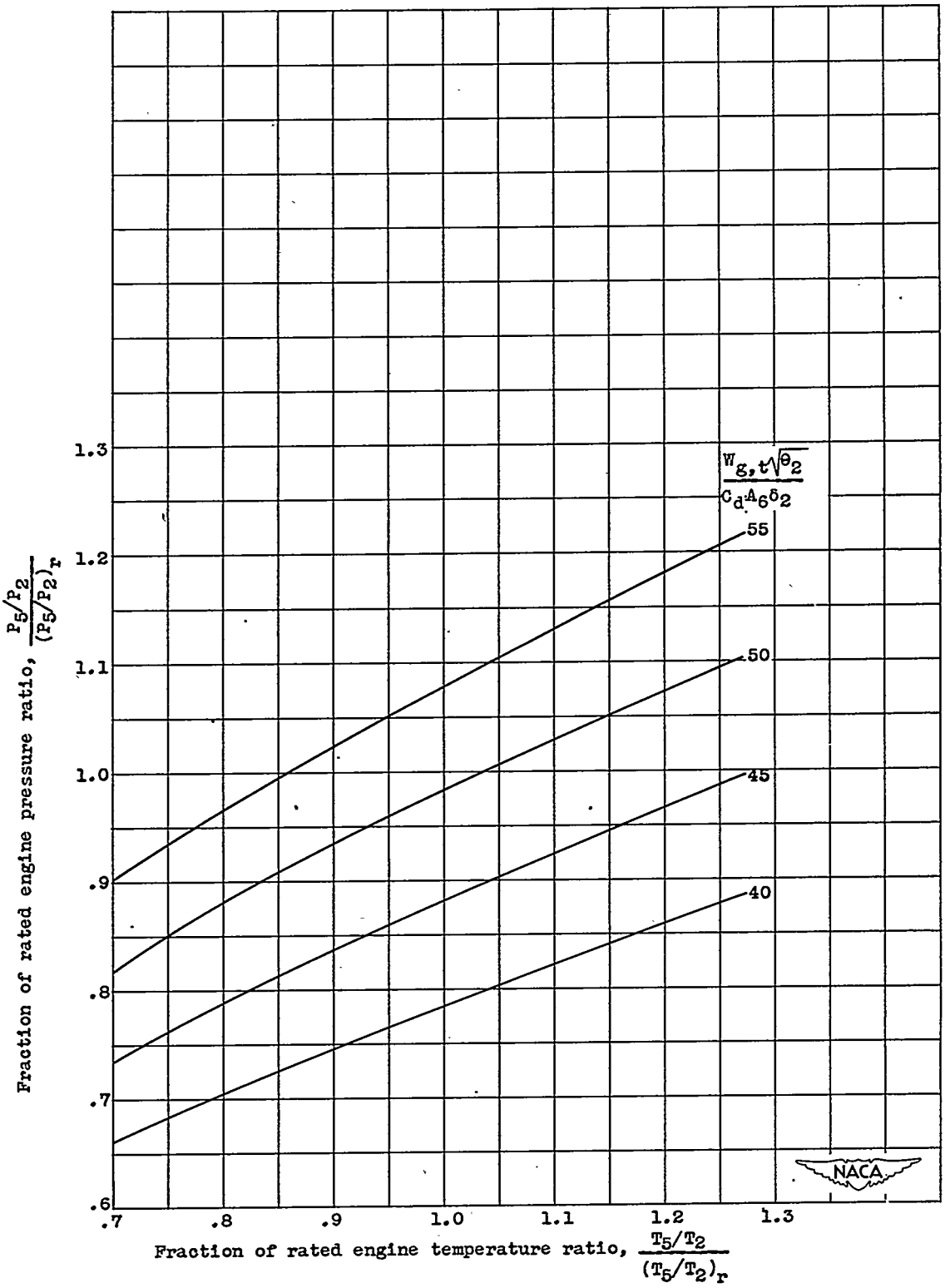


Figure 8. - Tail-pipe-nozzle characteristics for ram pressure ratio of 1.35.

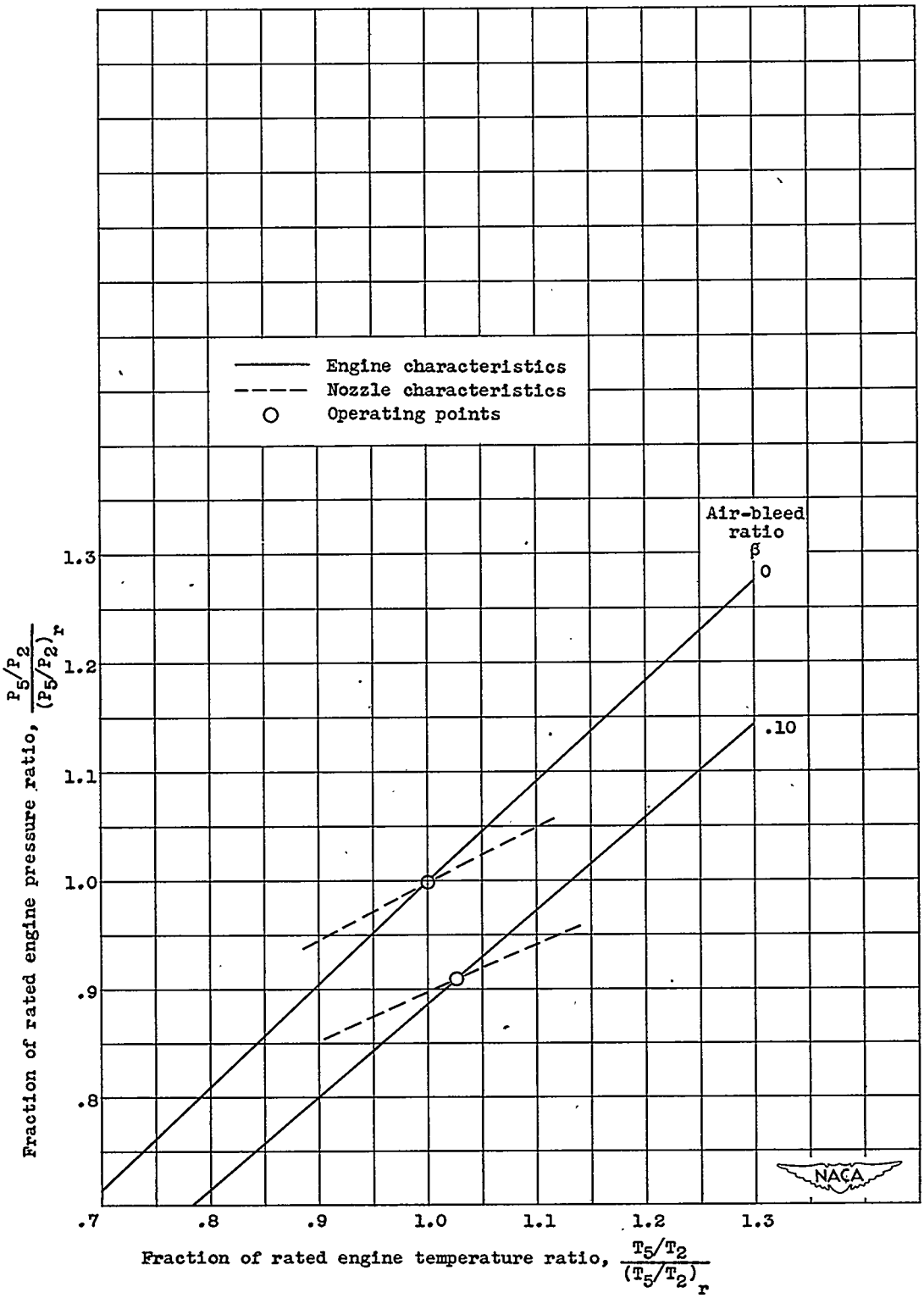


Figure 9. - Determination of operating points by intersection of pumping characteristics and nozzle characteristics for rated engine speed using standard-area choked tail-pipe nozzle. Ram pressure ratio, 1.35.

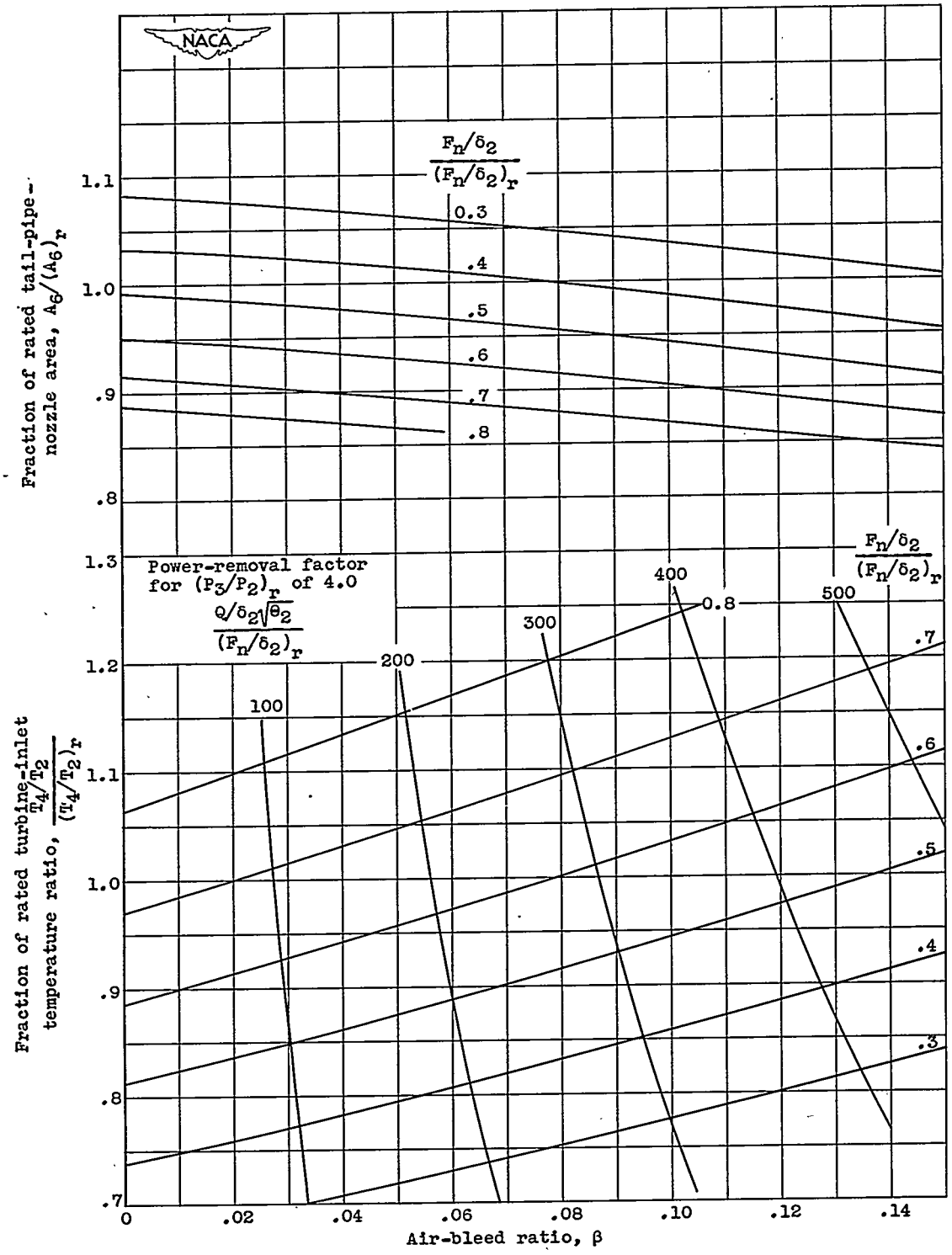


(a) Corrected engine speed, 0.9 rated.

Figure 10. - Variation of tail-pipe-nozzle area, turbine-inlet temperature ratio, and power-removal factor with air bleed and thrust for variable-area tail-pipe nozzle and ram pressure ratio of 1.35.

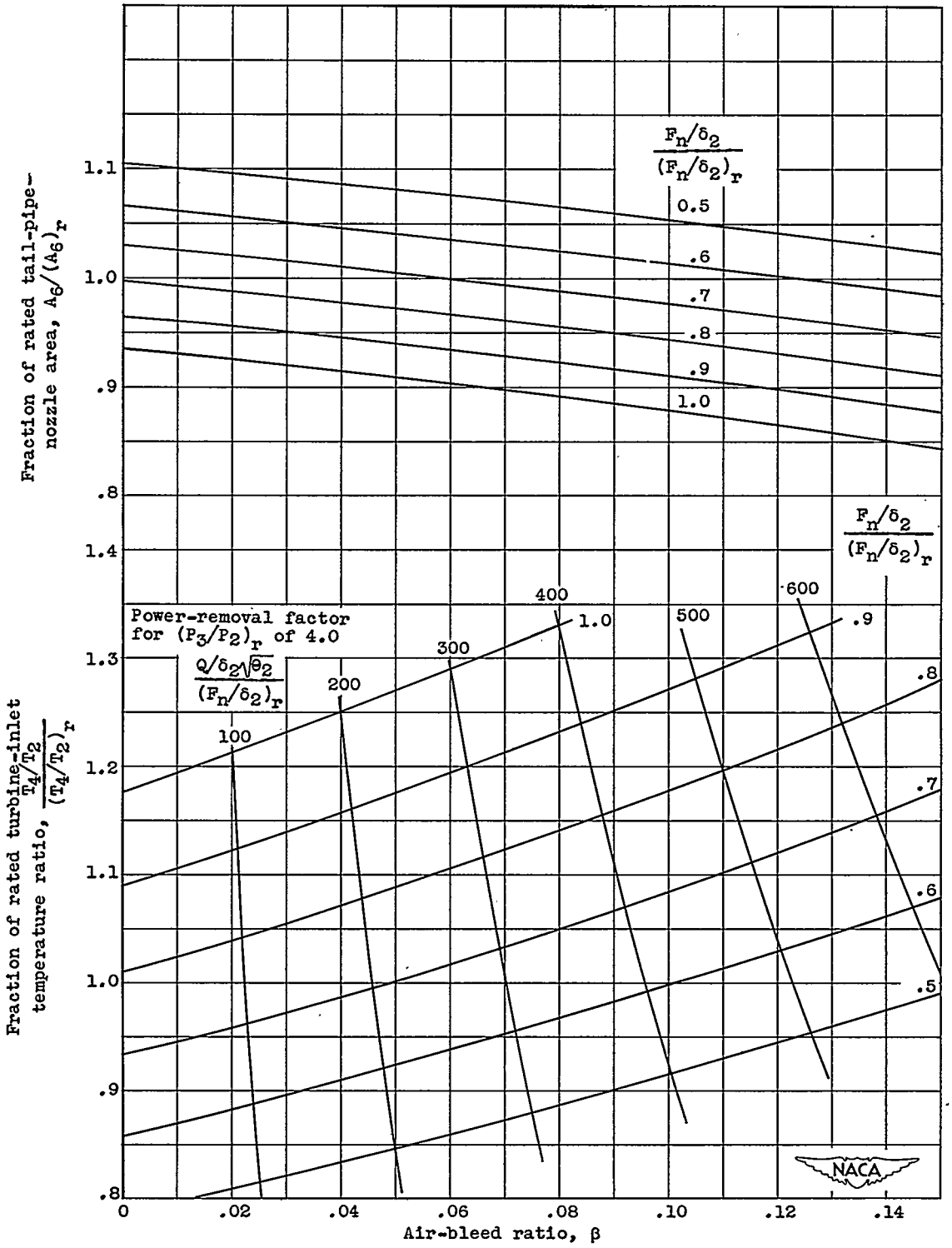


(b) Corrected engine speed, rated.

Figure 10. - Continued. Variation of tail-pipe-nozzle area, turbine-inlet temperature ratio, and power-removal factor with air bleed and thrust for variable-area tail-pipe nozzle and ram pressure ratio of 1.35.

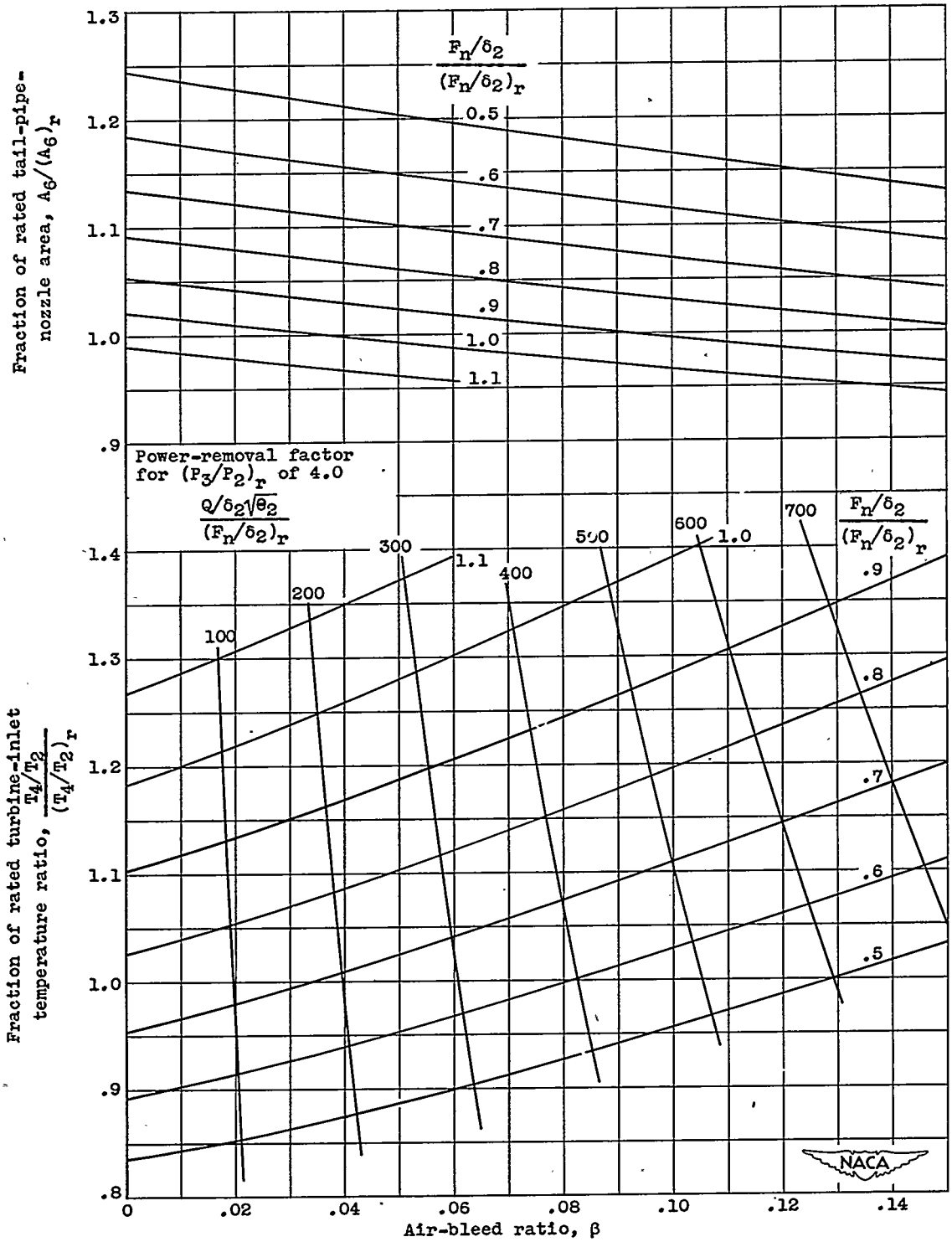


(c) Corrected engine speed, 1.1 rated.

Figure 10. - Concluded. Variation of tail-pipe-nozzle area, turbine-inlet temperature ratio, and power-removal factor with air bleed and thrust for variable-area tail-pipe nozzle and ram pressure ratio of 1.35.

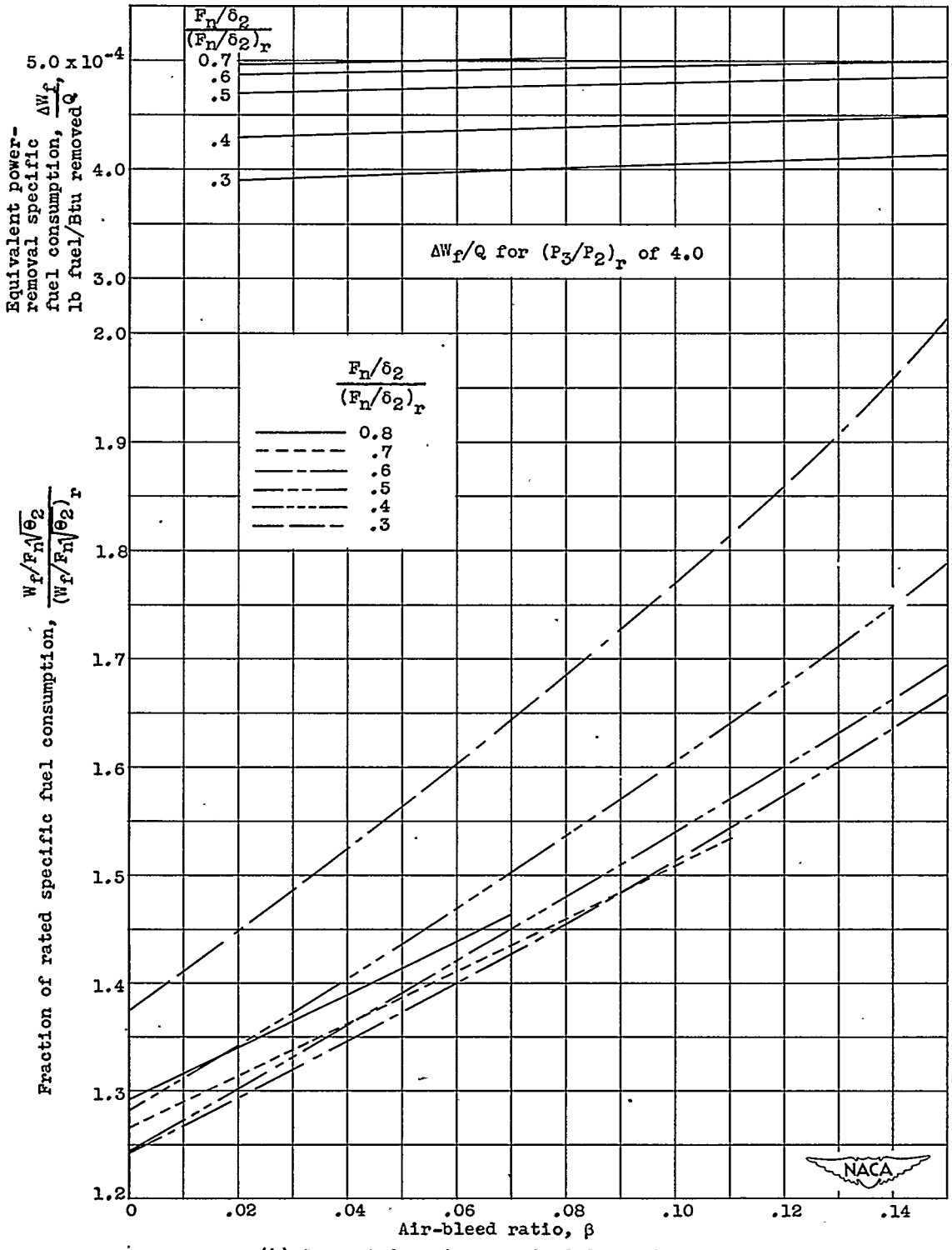


(á) Corrected engine speed, 0.9 rated.

Figure 11. - Variation of specific fuel consumption with air bleed and thrust for variable-area tail-pipe nozzle and ram pressure ratio of 1.35.

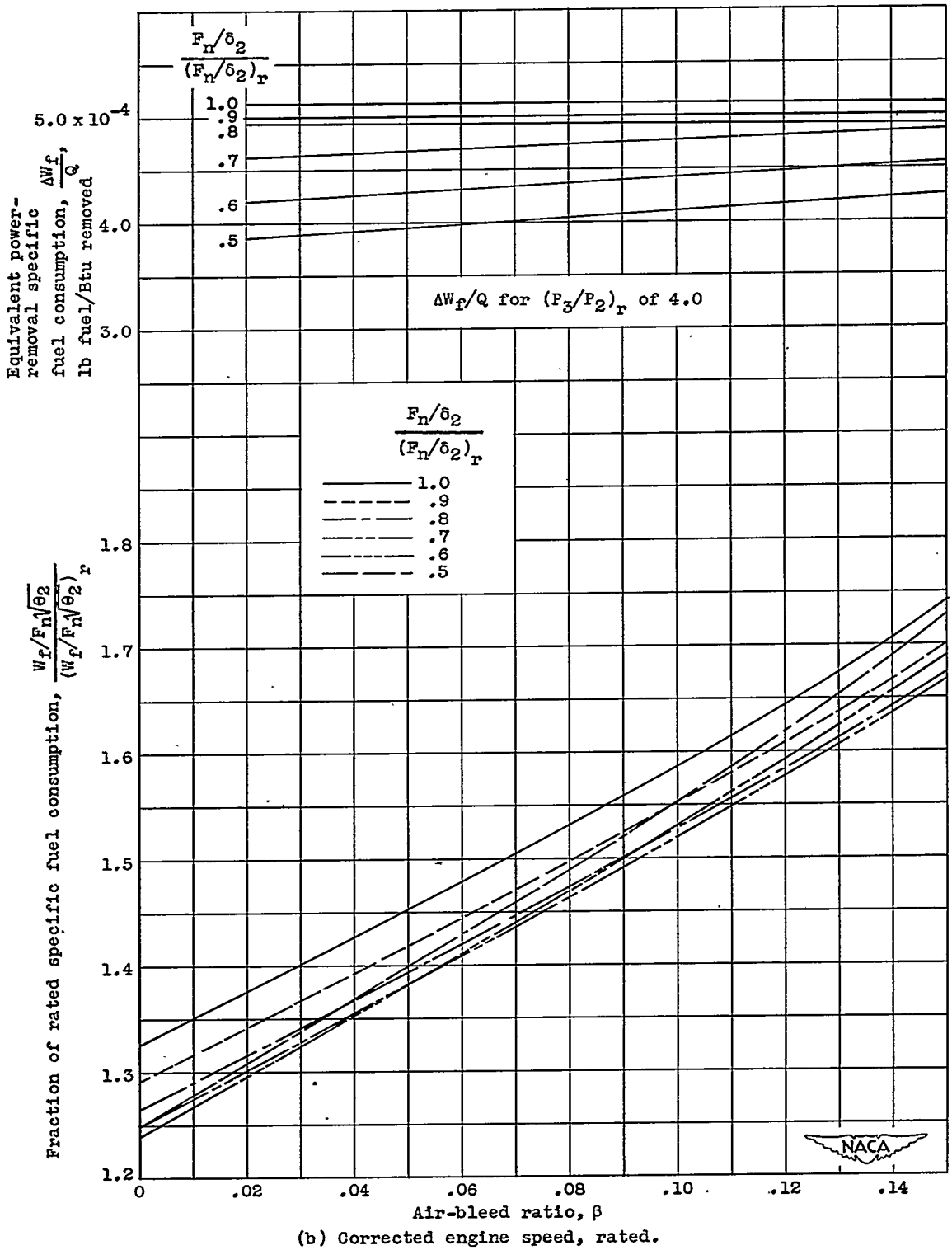


(b) Corrected engine speed, rated.

Figure 11. - Continued. Variation of specific fuel consumption with air bleed and thrust for variable-area tail-pipe nozzle and ram pressure ratio of 1.35.

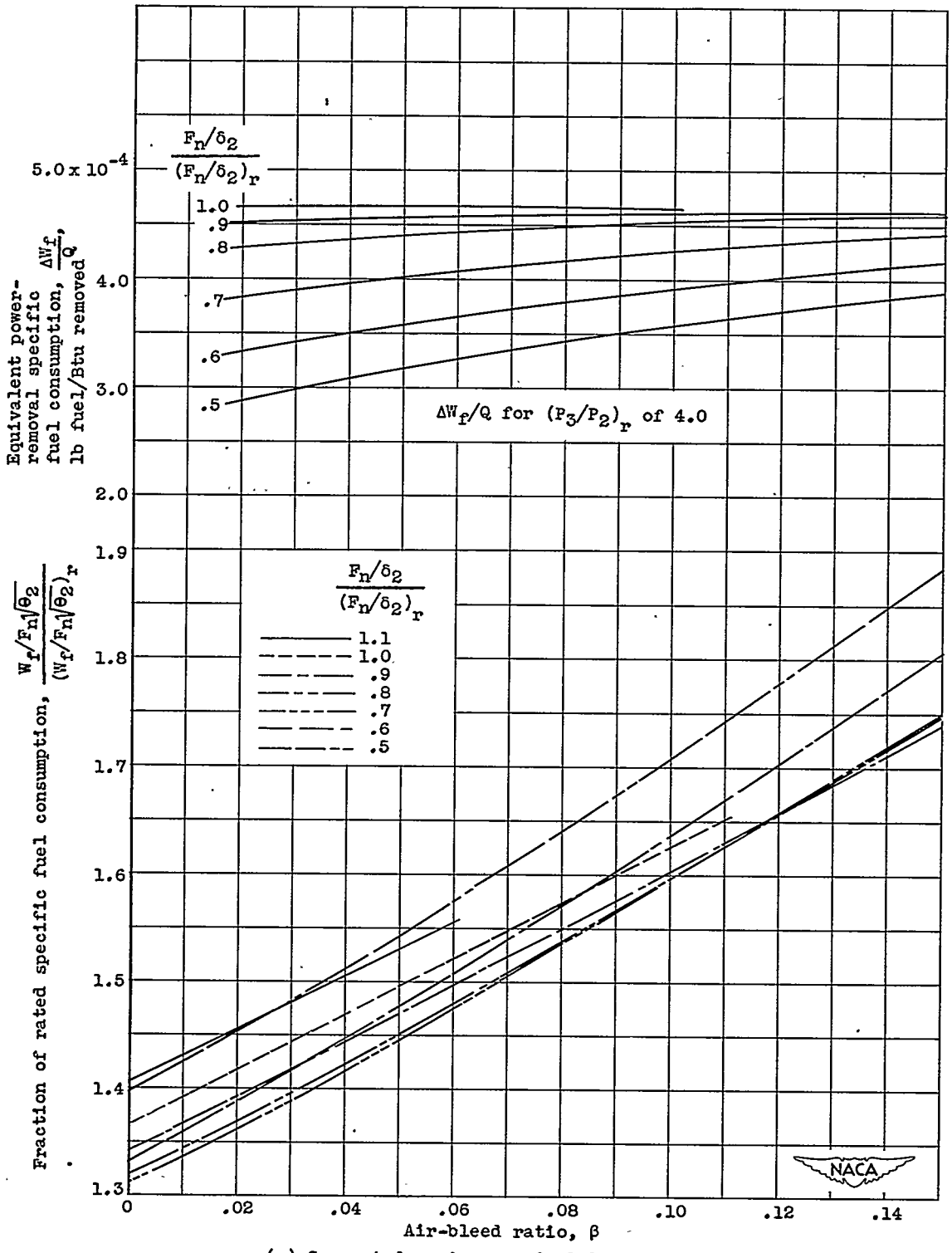


(c) Corrected engine speed, 1.1 rated.

Figure 11. - Concluded. Variation of specific fuel consumption with air bleed and thrust for variable-area tail-pipe nozzle and ram pressure ratio of 1.35.

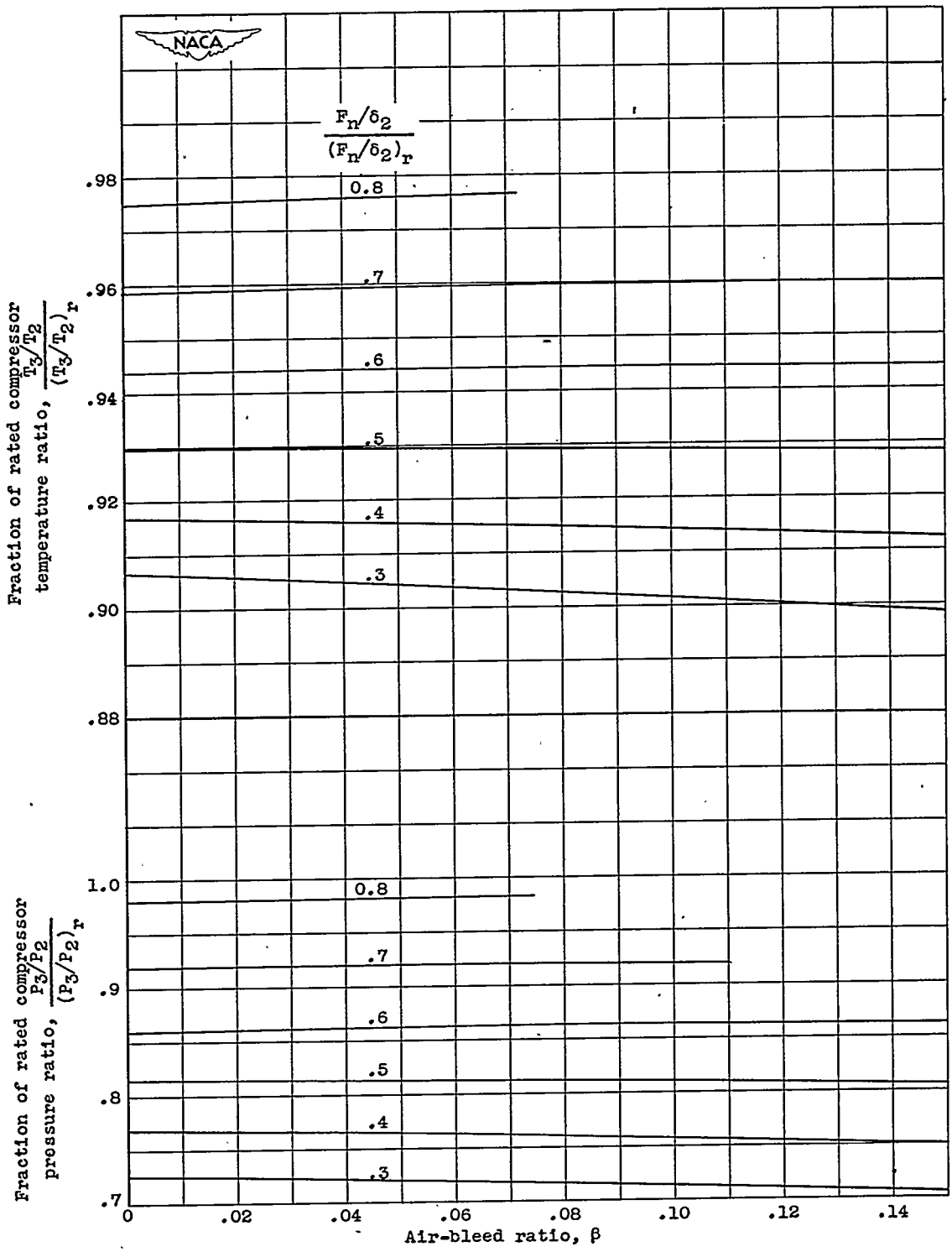


(a) Corrected engine speed, 0.9 rated.

Figure 12. - Variation of compressor temperature ratio and compressor pressure ratio with air bleed and thrust for variable-area tail-pipe nozzle and ram pressure ratio of 1.35.

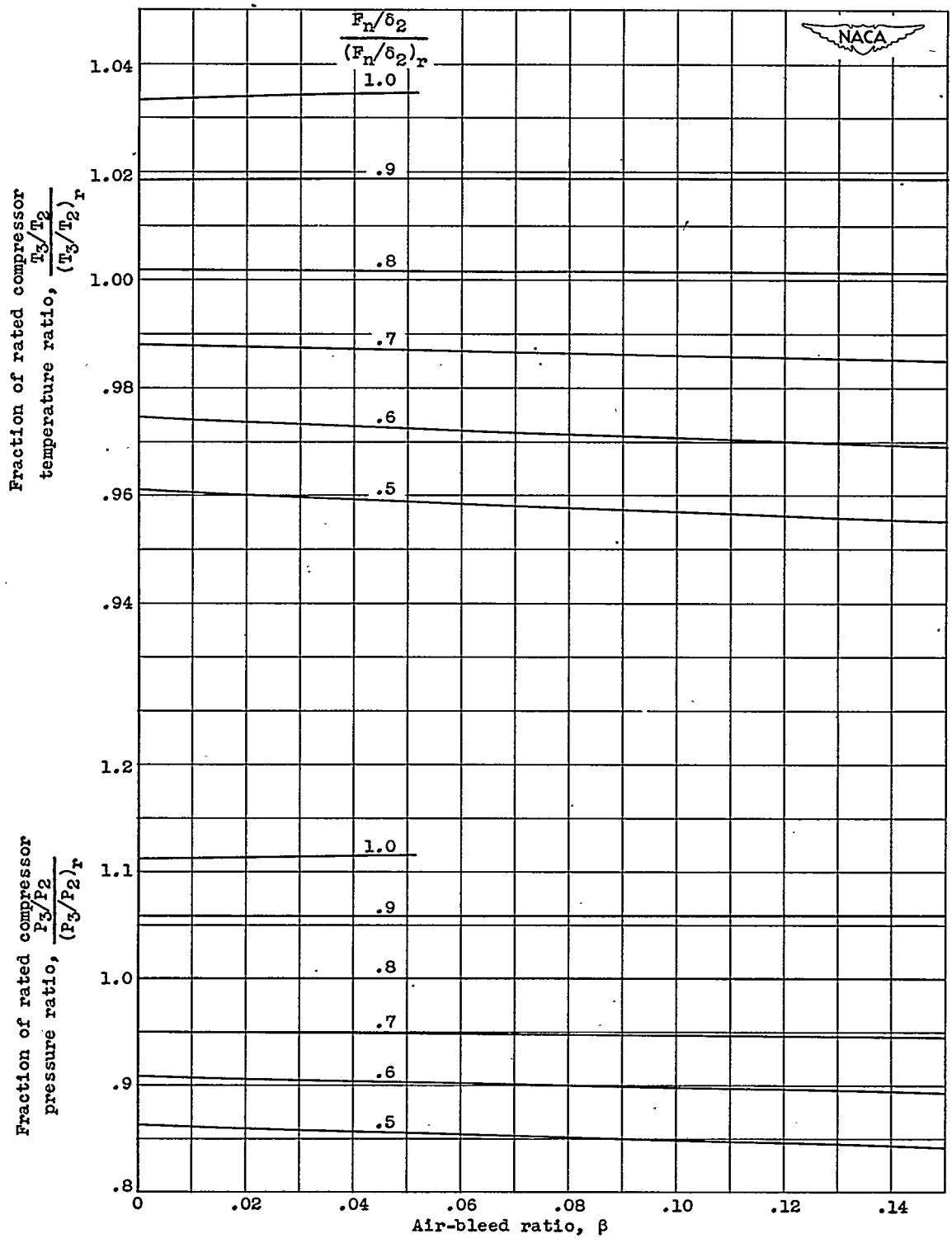


(b) Corrected engine speed, rated.

Figure 12. - Continued. Variation of compressor temperature ratio and compressor pressure ratio with air bleed and thrust for variable-area tail-pipe nozzle and ram pressure ratio of 1.35.

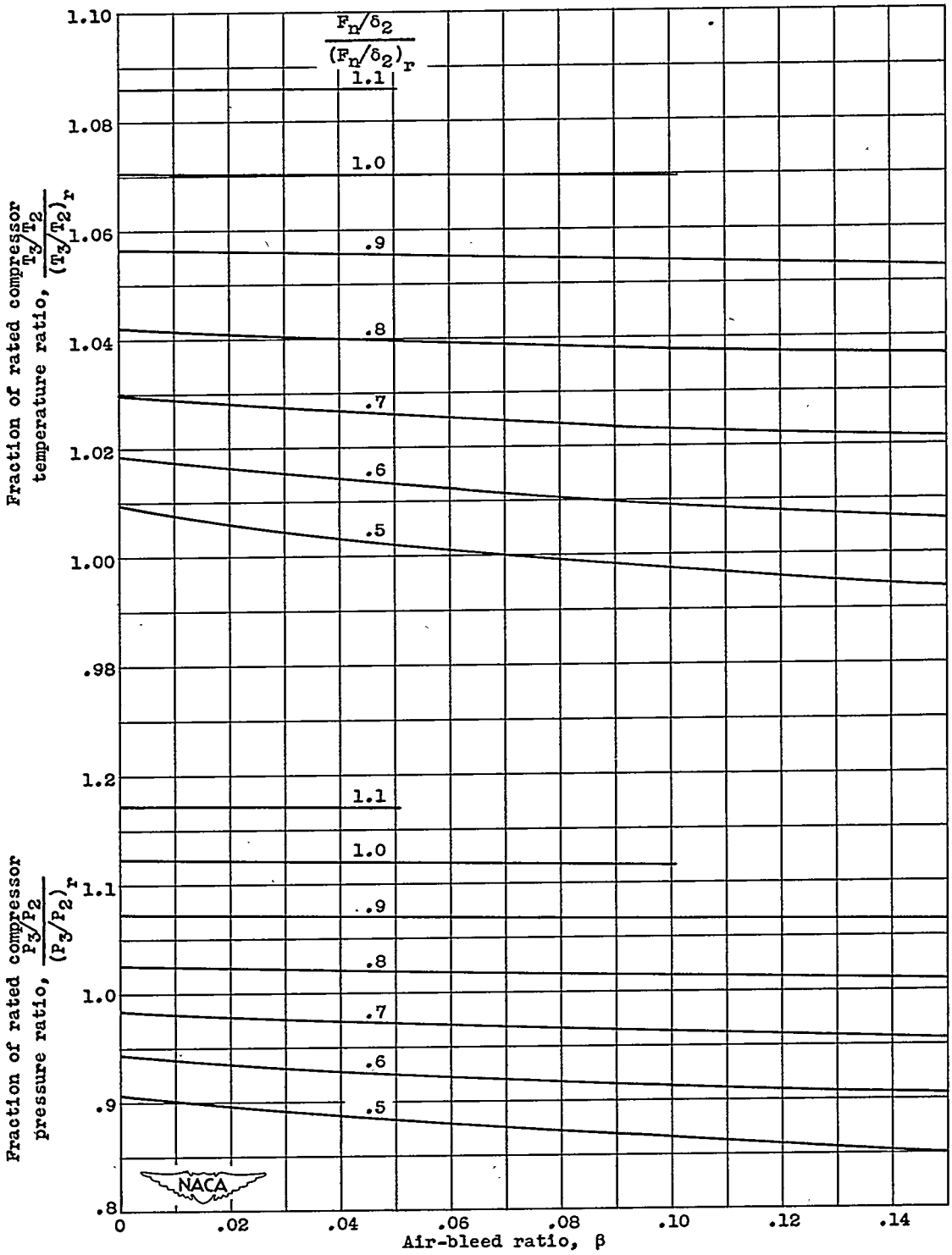


(c) Corrected engine speed, 1.1 rated.

Figure 12. - Concluded. Variation of compressor temperature ratio and compressor pressure ratio with air bleed and thrust for variable-area tail-pipe nozzle and ram pressure ratio of 1.35.

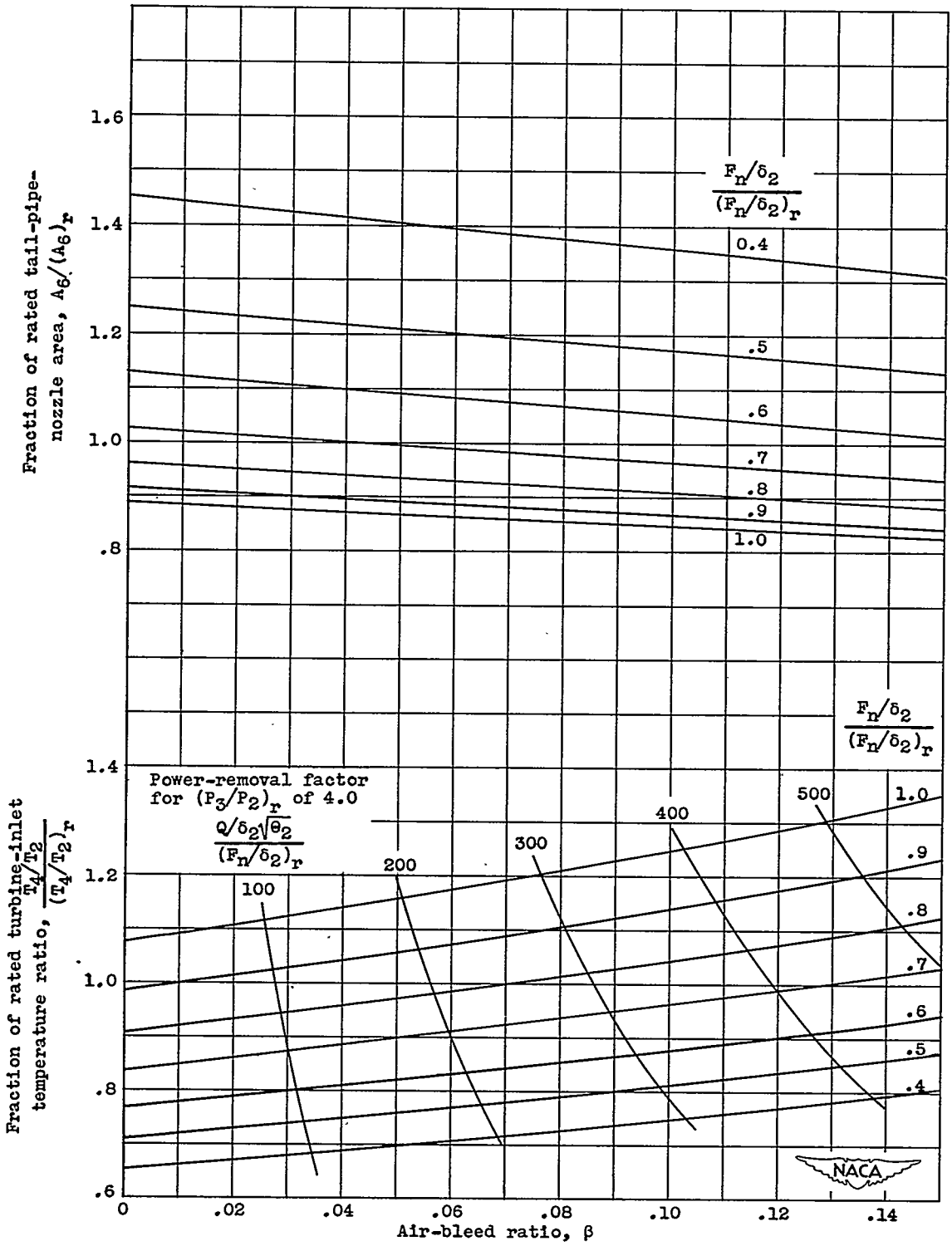


(a) Corrected engine speed, 0.9 rated.

Figure 13. - Variation of tail-pipe-nozzle area, turbine-inlet temperature ratio, and power-removal factor with air bleed and thrust for variable-area tail-pipe nozzle and ram pressure ratio of 0.99.

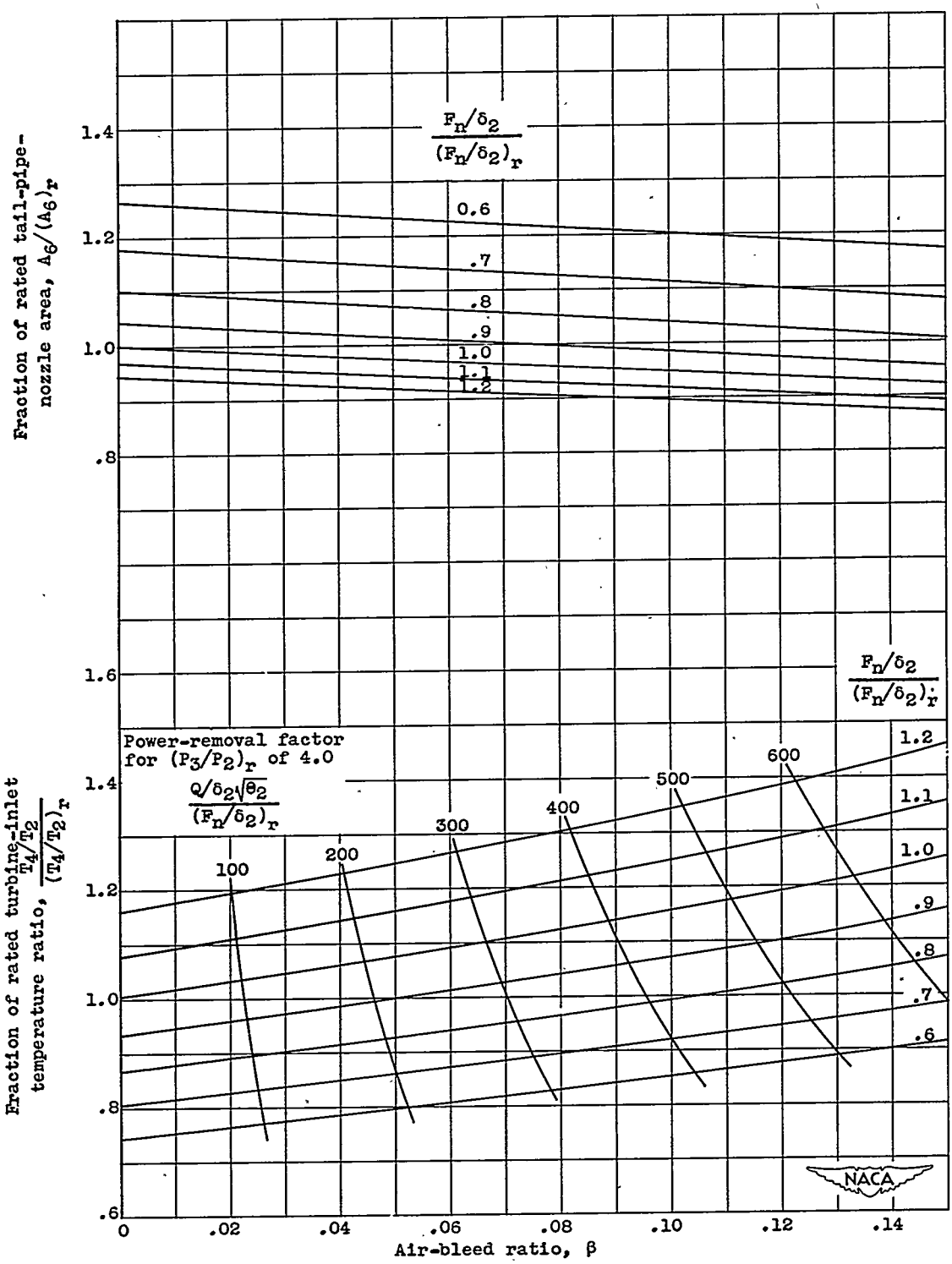


(b) Corrected engine speed, rated.

Figure 13. - Continued. Variation of tail-pipe-nozzle area, turbine-inlet temperature ratio, and power-removal factor with air bleed and thrust for variable-area tail-pipe nozzle and ram pressure ratio of 0.99.

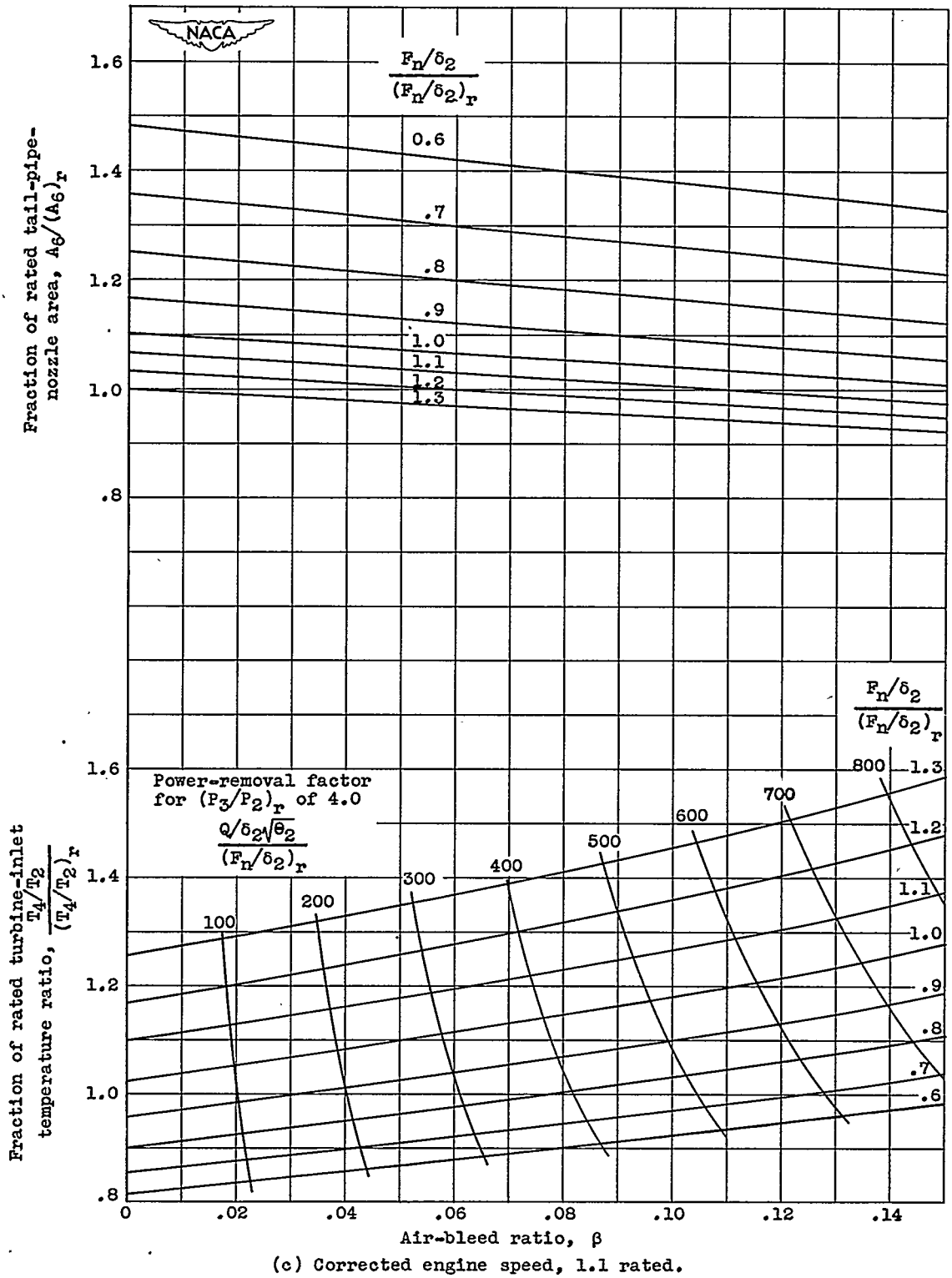


(c) Corrected engine speed, 1.1 rated.

Figure 13. - Concluded. Variation of tail-pipe-nozzle area, turbine-inlet temperature ratio, and power-removal factor with air bleed and thrust for variable-area tail-pipe nozzle and ram pressure ratio of 0.99.

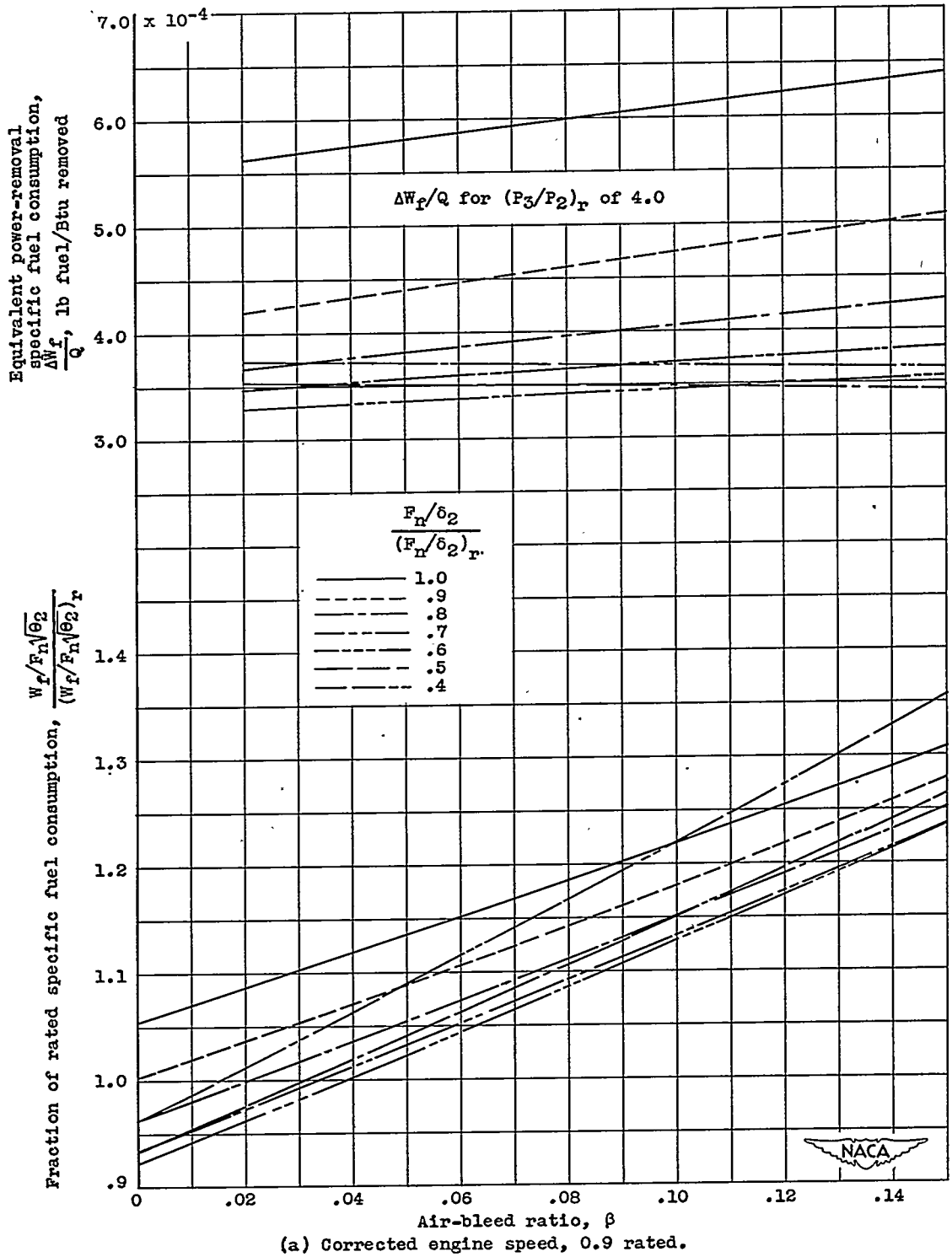


(a) Corrected engine speed, 0.9 rated.

Figure 14. - Variation of specific fuel consumption with air bleed and thrust for variable-area tail-pipe nozzle and ram pressure ratio of 0.99.

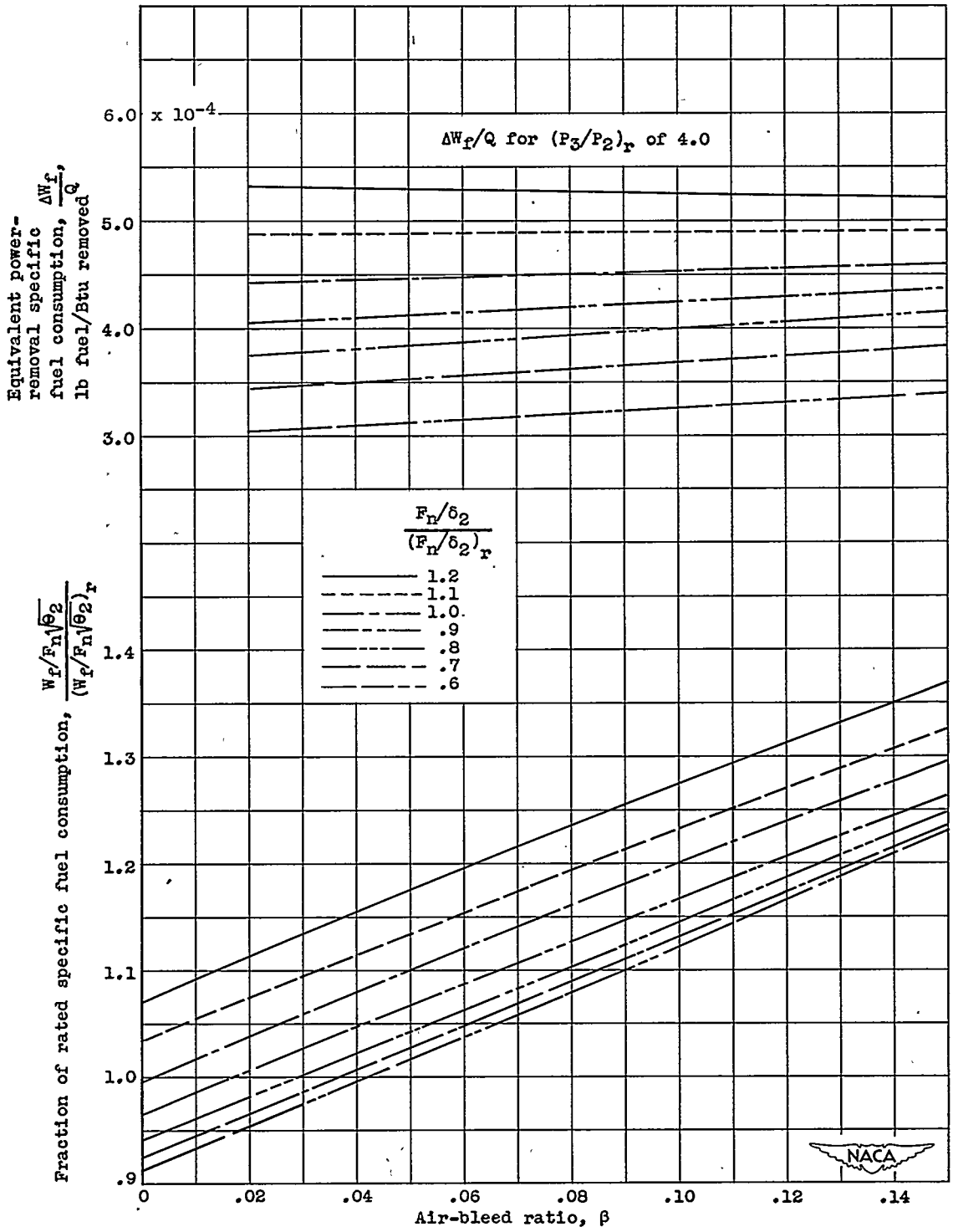


(b) Corrected engine speed, rated.

Figure 14. - Continued. Variation of specific fuel consumption with air bleed and thrust for variable-area tail-pipe nozzle and ram pressure ratio of 0.99.

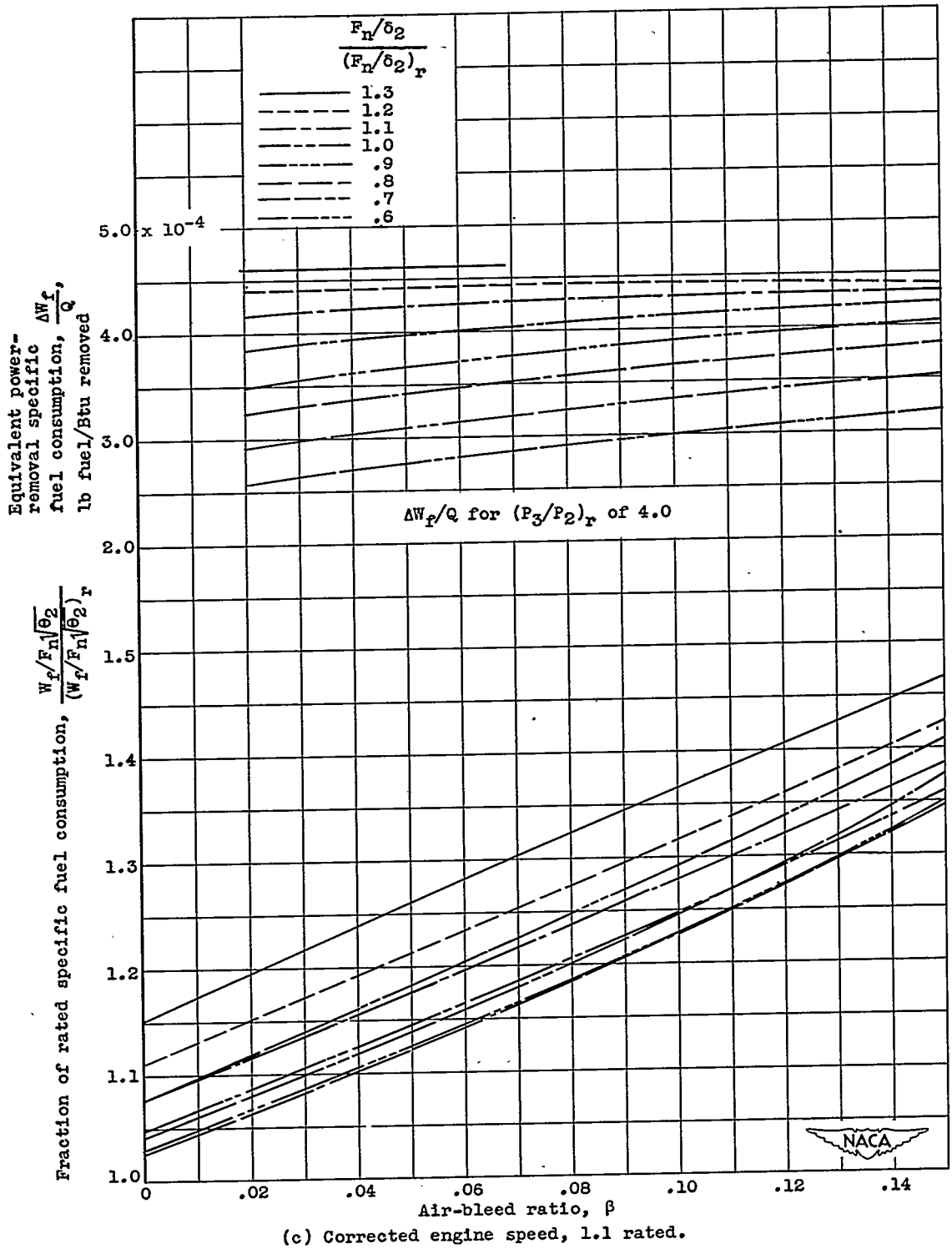


(c) Corrected engine speed, 1.1 rated.

Figure 14. - Concluded. Variation of specific fuel consumption with air bleed and thrust for variable-area tail-pipe nozzle and ram pressure ratio of 0.99.

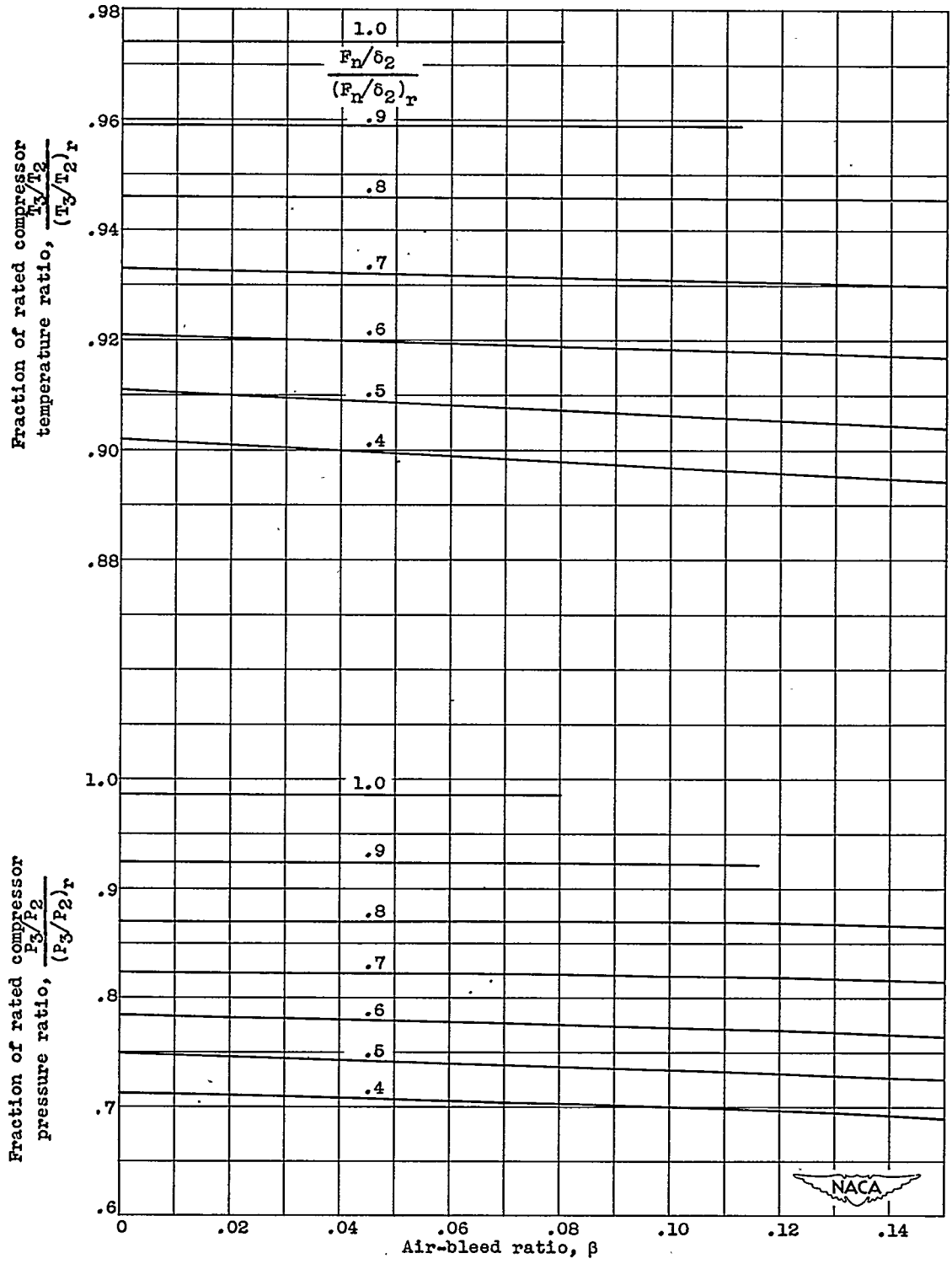


(a) Corrected engine speed, 0.9 rated.

Figure 15. - Variation of compressor temperature ratio and compressor pressure ratio with air bleed and thrust for variable-area tail-pipe nozzle and ram pressure ratio of 0.99.

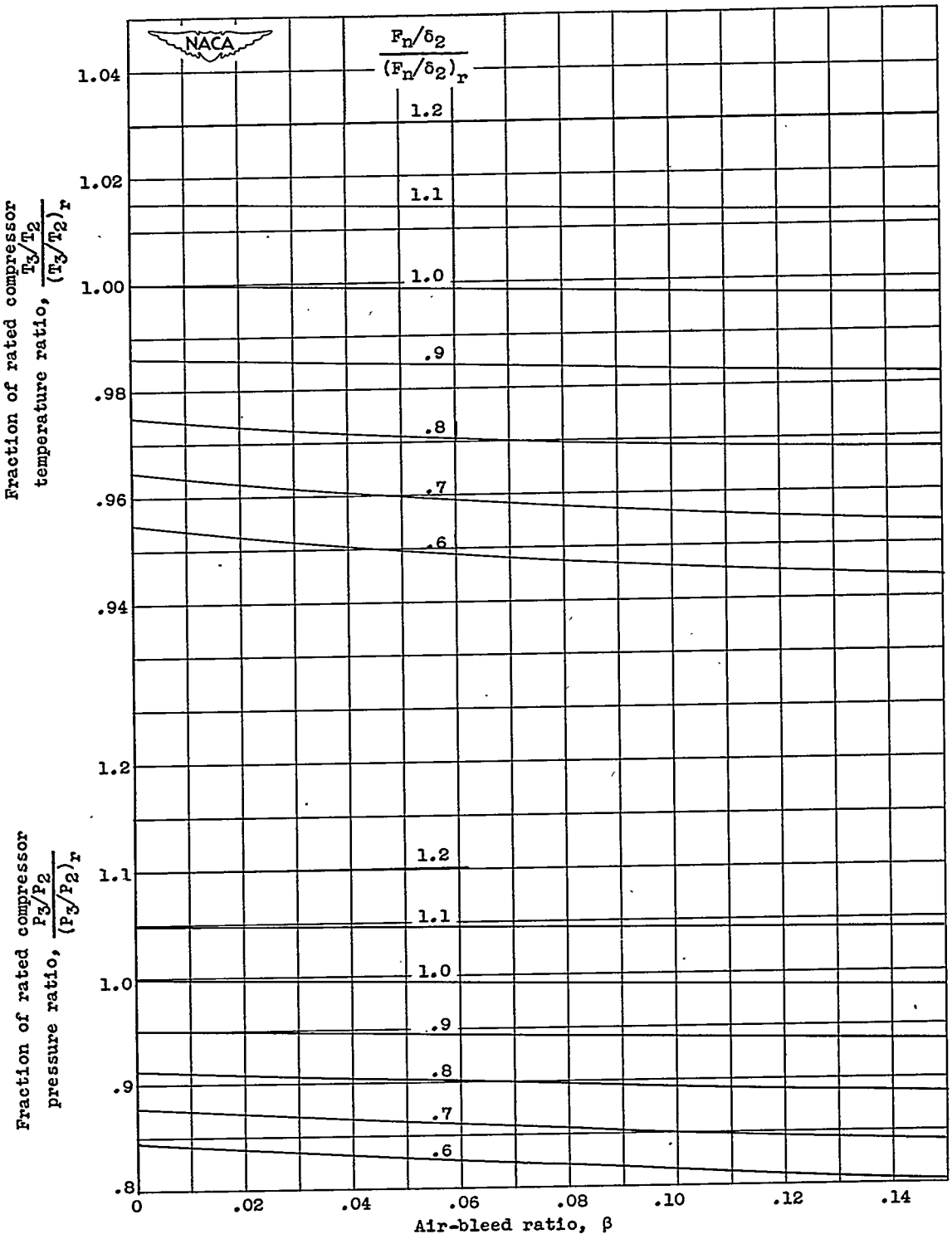


(b) Corrected engine speed, rated.

Figure 15. - Continued. Variation of compressor temperature ratio and compressor pressure ratio with air bleed and thrust for variable-area tail-pipe nozzle and ram pressure ratio of 0.99.

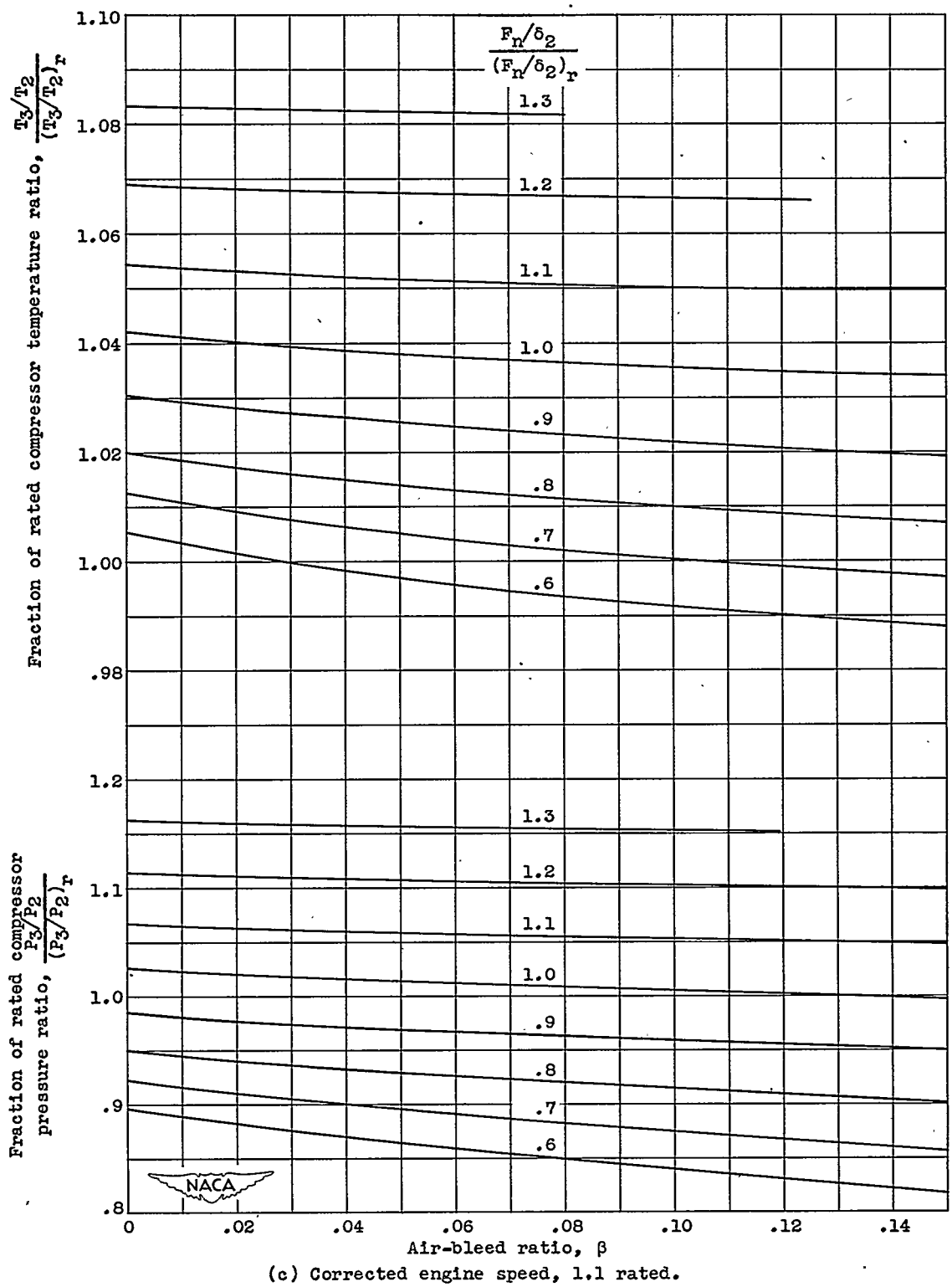


(c) Corrected engine speed, 1.1 rated.

Figure 15. - Concluded. Variation of compressor temperature ratio and compressor pressure ratio with air bleed and thrust for variable-area tail-pipe nozzle and ram pressure ratio of 0.99.

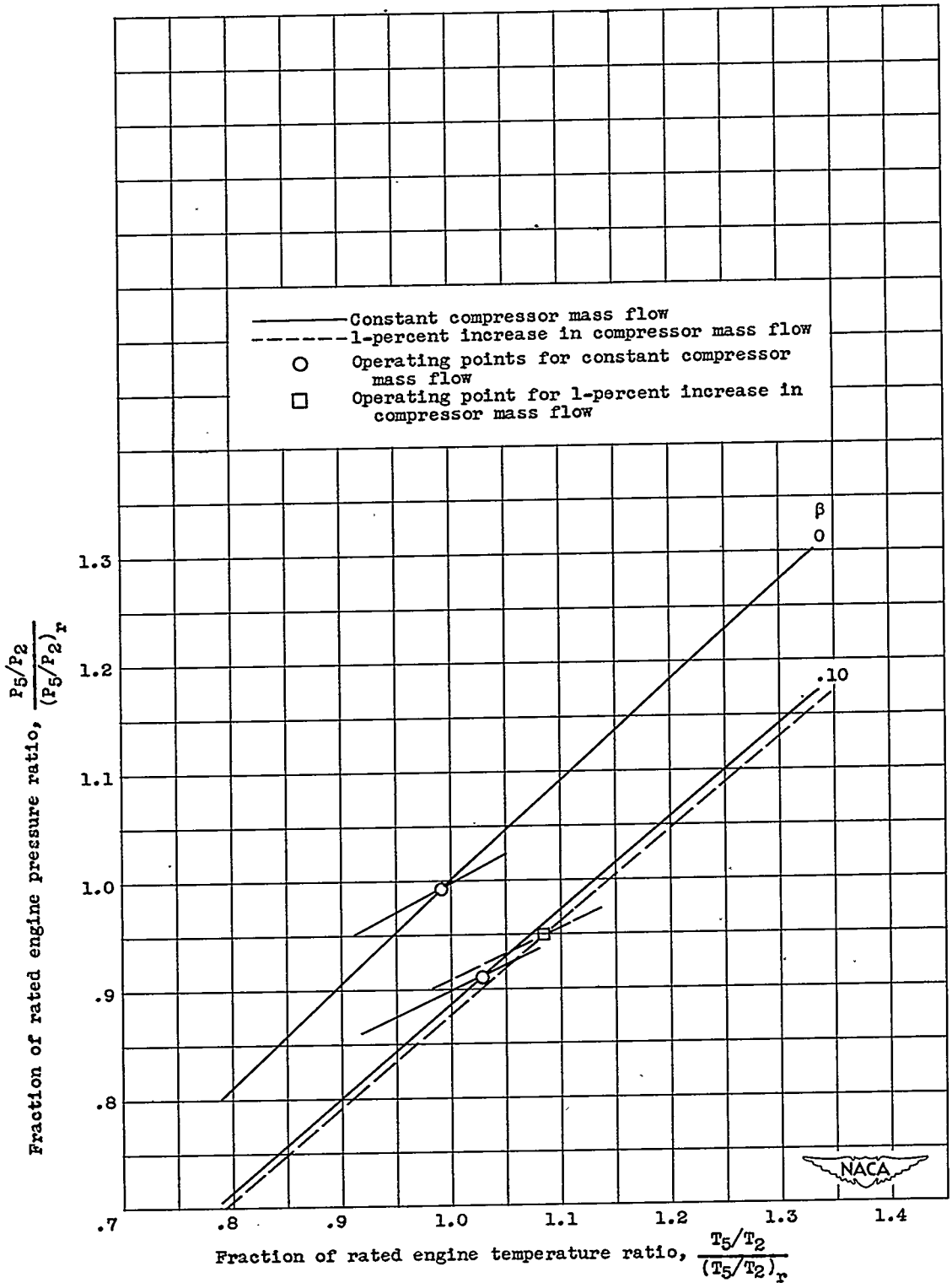


Figure 16. - Illustration of change in constant-area operating points with 1-percent increase in compressor mass flow. Corrected engine speed, rated; ram pressure ratio, 1.35.

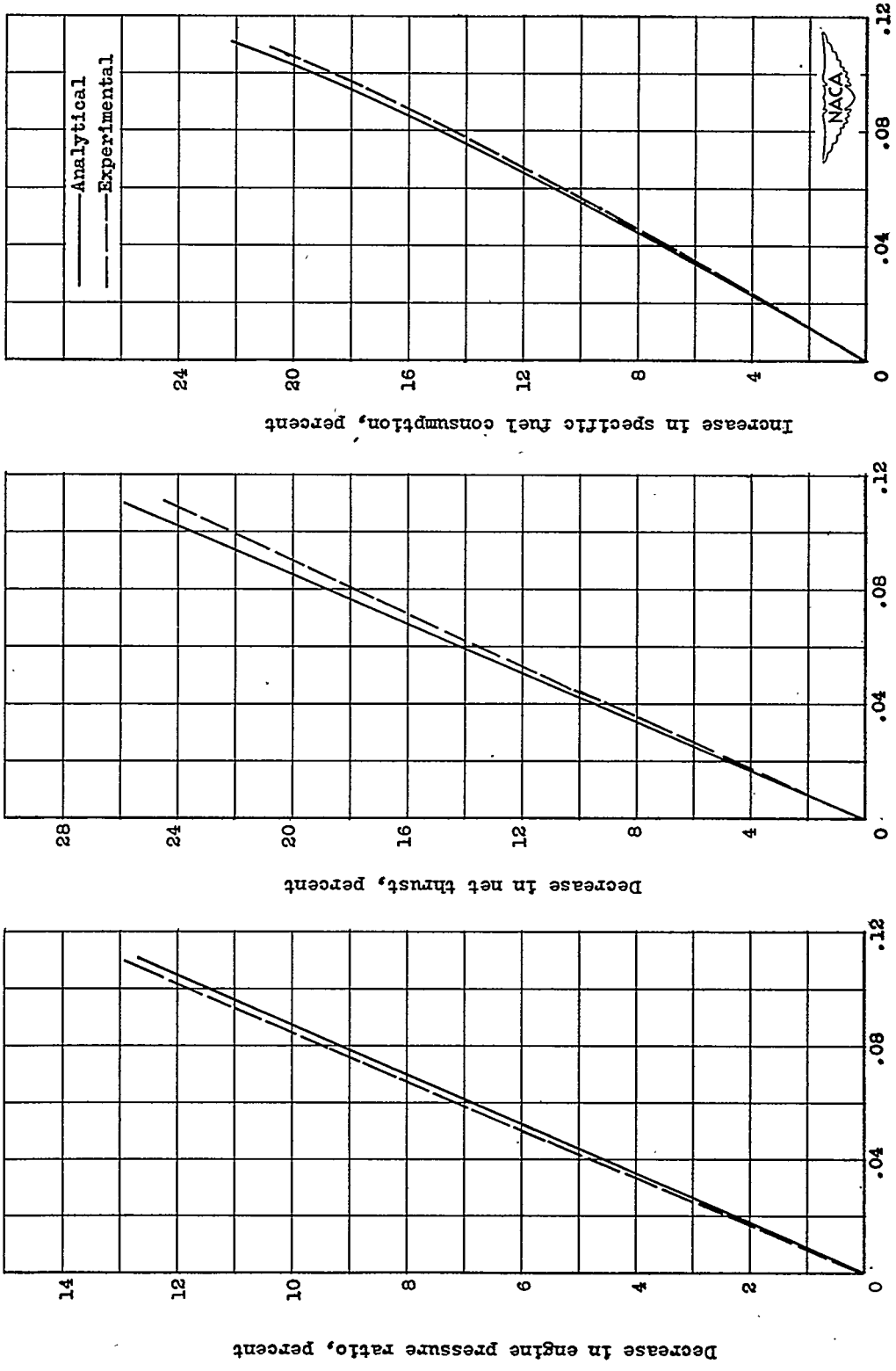


(a) Corrected engine speed, 0.91 rated; engine temperature ratio, rated.

Figure 17. - Comparison of analytical and experimental results of air bleed at constant turbine-outlet temperature for ram pressure ratio of 1.2.

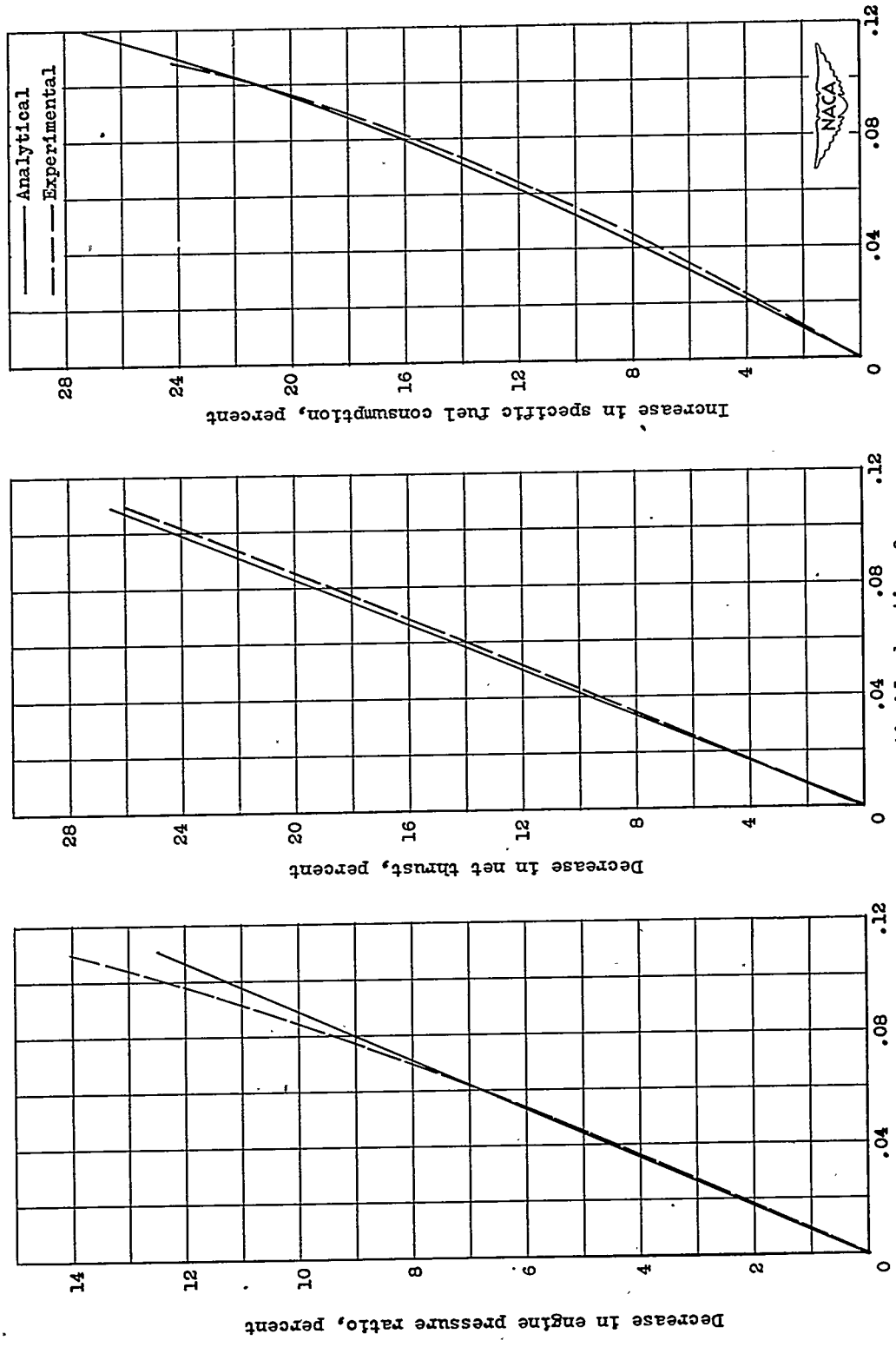


(b) Corrected engine speed, 1.03 rated; engine temperature ratio, rated.

Figure 17. - Concluded. Comparison of analytical and experimental results of air bleed at constant turbine-outlet temperature for ram pressure ratio of 1.2.

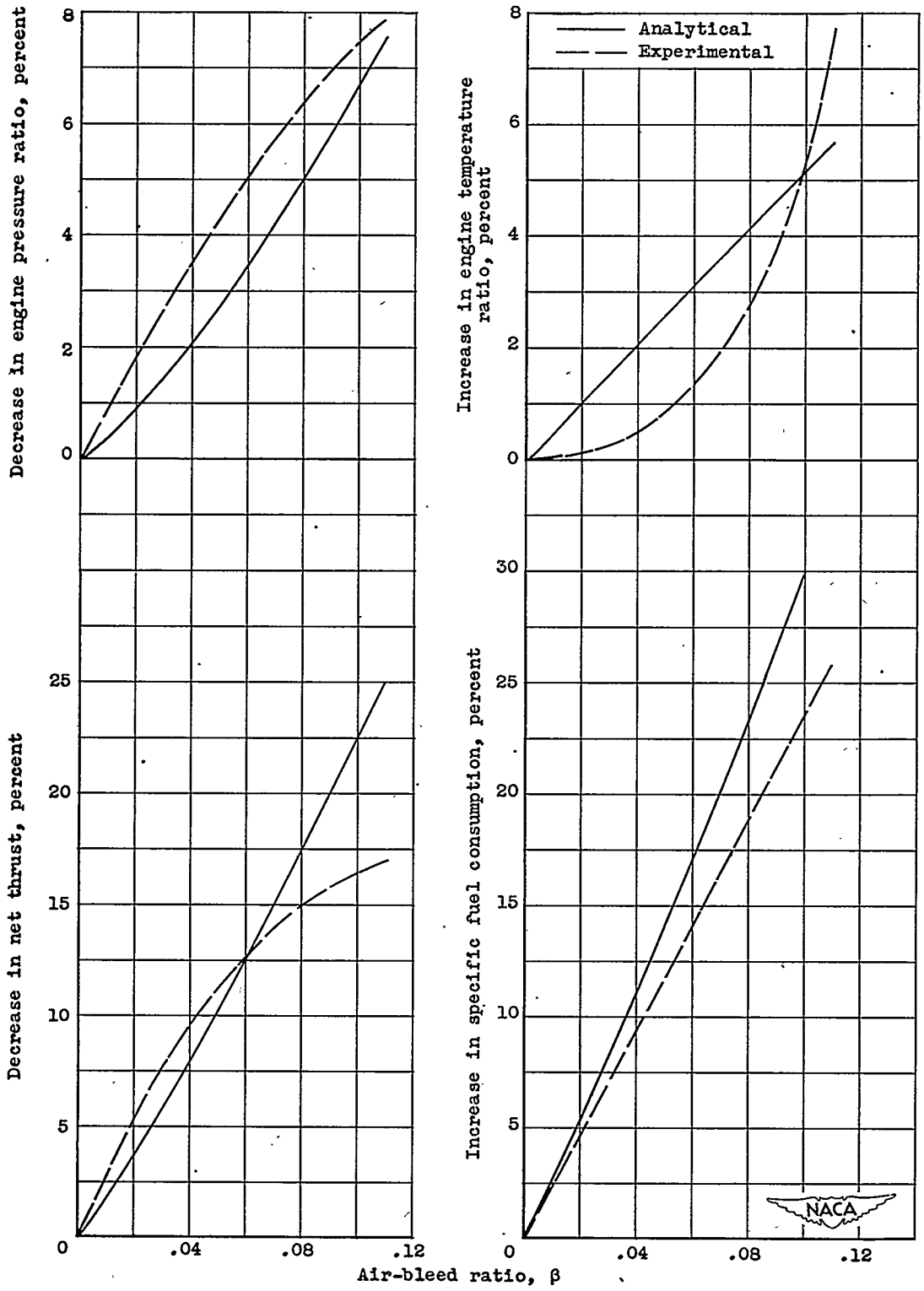


(a) Corrected engine speed, 0.91 rated; tail-pipe-nozzle area, rated.

Figure 18. - Comparison of analytical and experimental results of air bleed with constant tail-pipe-nozzle area for ram pressure ratio of 1.2.

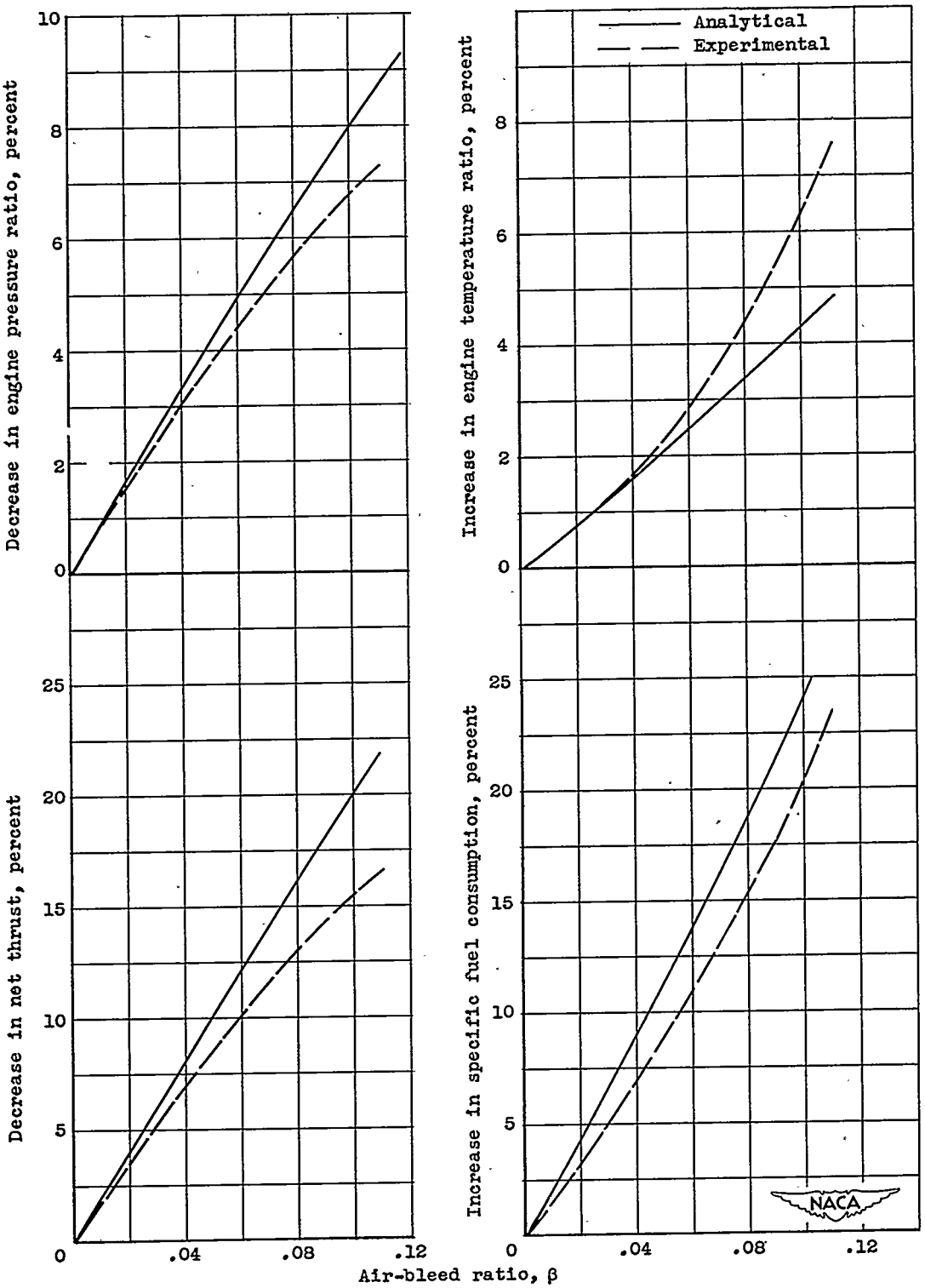


(b) Corrected engine speed, 1.03 rated; tail-pipe-nozzle area, 1.07 rated.

Figure 18. - Concluded. Comparison of analytical and experimental results of air bleed with constant tail-pipe-nozzle area for ram pressure ratio of 1.2.